Atomic-scale structure of disordered pharmaceutical materials by high-energy XRD and atomic PDF analysis

Valeri Petkov
Department of Physics, Central Michigan University, Mt. Pleasant, MI 48859
petkov@phy.cmich.edu

Help us improve Wikipedia by supporting it financially.

Sign in / create account

article | discussion | edit this page | history

Interested in contributing to Wikipedia?

WIKIPEDIA
The Free Encyclopedia

navigation
- Main page
- Contents
- Featured content
- Current events
- Random article

interaction
- About Wikipedia
- Community portal
- Recent changes
- Contact Wikipedia
- Donate to Wikipedia
- Help

search
Go Search

toolbox
- What links here
- Related changes
- Upload file
- Special pages
- Printable version
- Permanent link
- Cite this article

in other languages

Mount Pleasant, Michigan

From Wikipedia, the free encyclopedia

Mount Pleasant is a city that serves as the county seat of Isabella County[6] in the U.S. state of Michigan. As of the 2000 census, the city population was 25,946.

Part of the city (with a population of 8,741) is on the Isabella Indian Reservation, site of the Soaring Eagle Casino. The city is also home to the main campus of Central Michigan University. Former Michigan governor John Engler was born in Mount Pleasant.

Contents [hide]
1 Geography
2 Demographics
3 Places of interest
4 Local media
5 Sister cities
6 External links

Geography [edit]

According to the United States Census Bureau, the city has a total area of 20.2 km² (7.8 mi²), all land. The Chippewa River runs through the city. Mount Pleasant is located approximately 61 miles north of Lansing, Michigan's state capital, along US 127.

Demographics [edit]

As of the census² of 2000, there were 25,946 people, 8,449 households, and 3,126 families residing in the city. The population density was 1,284.3/km² (3,327.2/mi²). There were 8,878 housing units at an average density of 439.5/km² (1,138.5/mi²). The racial makeup of the city was 89.12% White, 3.67% African American, 1.54% Native American, 2.85% Asian, 0.07% Pacific Islander, 0.93% from other races, and 1.83% from two or more races. Hispanic or Latino of any race were 2.49% of the population.

Mount Pleasant, Michigan

Seal

Location in Isabella County the state of Michigan
Coordinates: 43°35'52.71"N 84°46'3.75"W

Country	United States
State	Michigan
County	Isabella County

This document was presented at PPXRD - Pharmaceutical Powder X-ray Diffraction Symposium

Sponsored by The International Centre for Diffraction Data

PPXRD Website – www.icdd.com/ppxrd

ICDD Website - www.icdd.com

Why do materials behave the way they do ? It has a lot to do with how atoms are arranged in materials, i.e. with the atomic-scale "structure", and that is why we need to know it well.

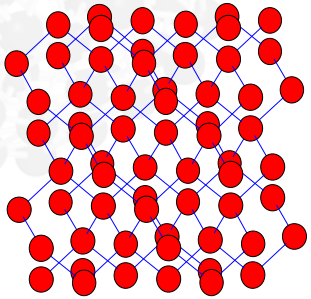

Diamond (crystal) - *hard, transparent, insulating and expensive.*

It is all just Carbon

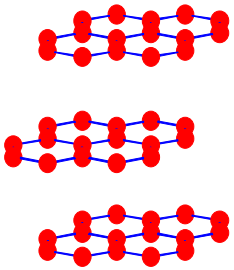

Graphite (crystal) - *soft, black, conducts heat and electricity and cheap.*

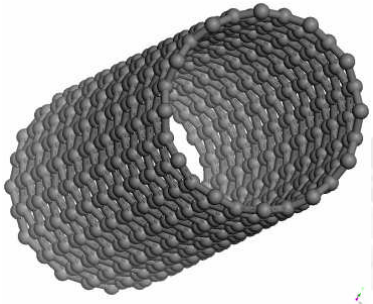

Carbon nanotubes
Stronger than steel

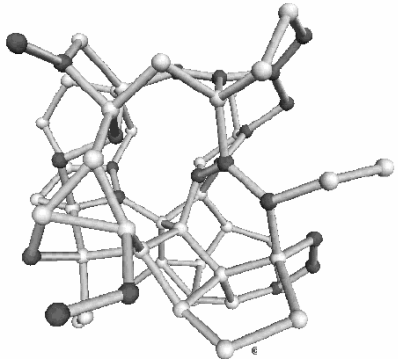

Amorphous Carbon
Catalysis

Atomic ordering in materials is determined by X-ray diffraction: Principles

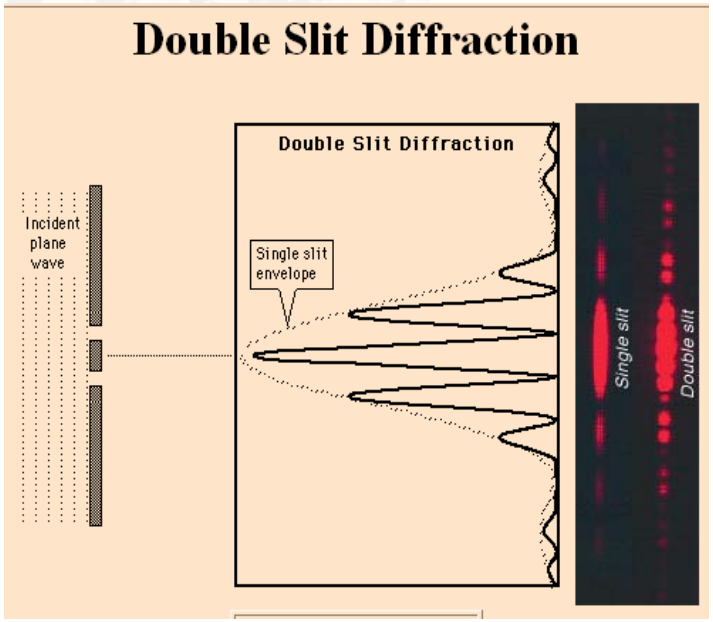

PHY 101: Diffraction of light

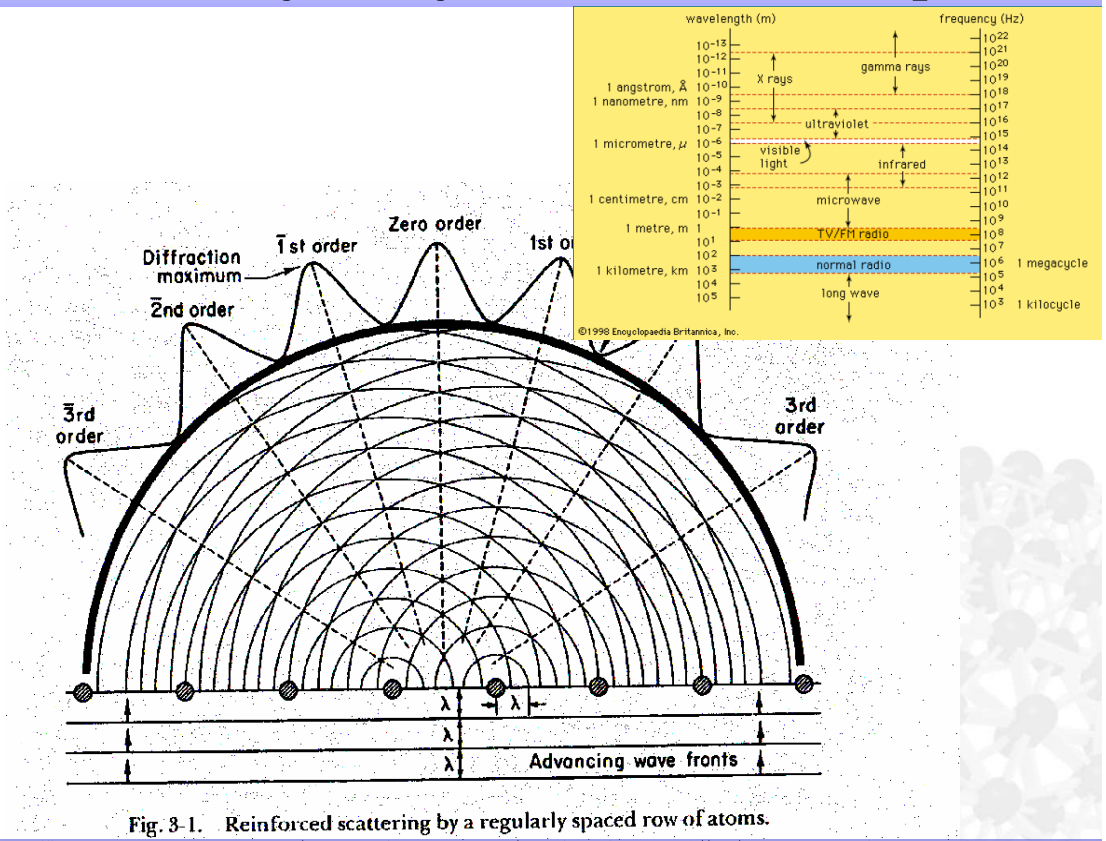

Fig. 3-1. Reinforced scattering by a regularly spaced row of atoms.

CRYST 101: Diffraction of x-rays from a single row of atoms (Klug and Alexander in "X-ray diffraction procedures")

Diffraction from Crossed Slits

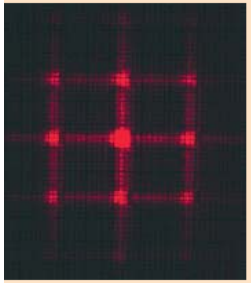

Appearance of object.

The diffraction pattern at left is formed by passing the light from a helium-neon laser through short slits which cross at a 90° angle, like a plus sign. The basic geometry is shown below.

This pattern shows that the diffraction pattern reveals the symmetry of the object from which it is diffracted. The 90° angles in the object are shown by 90° angles in the diffraction pattern. The spaces between the bright concentrations of light are inversely proportional to the widths of the slits forming the object, and could be used to measure those widths.

Conceptually, this is similar to using x-ray diffraction to reveal the symmetry and lattice spacings of the atoms in a crystal lattice.

Note: The diffraction pattern was projected upon a piece of graph paper - that accounts for the dark lines. They are not a part of the diffraction.

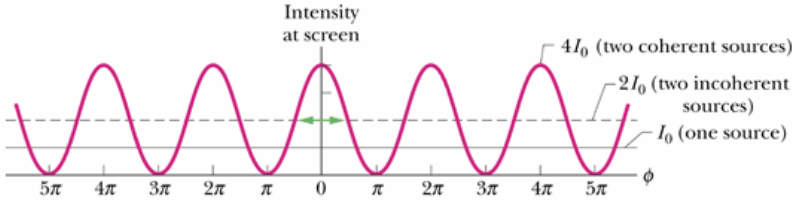

$$I = 4I_0 \cos^2 \frac{1}{2}\phi,$$

$$\phi = \frac{2\pi d}{\lambda} \sin\theta .$$

No Intensity loss, just Intensity re-distribution !

Structure of long-range (μm-range) ordered materials: Crystals

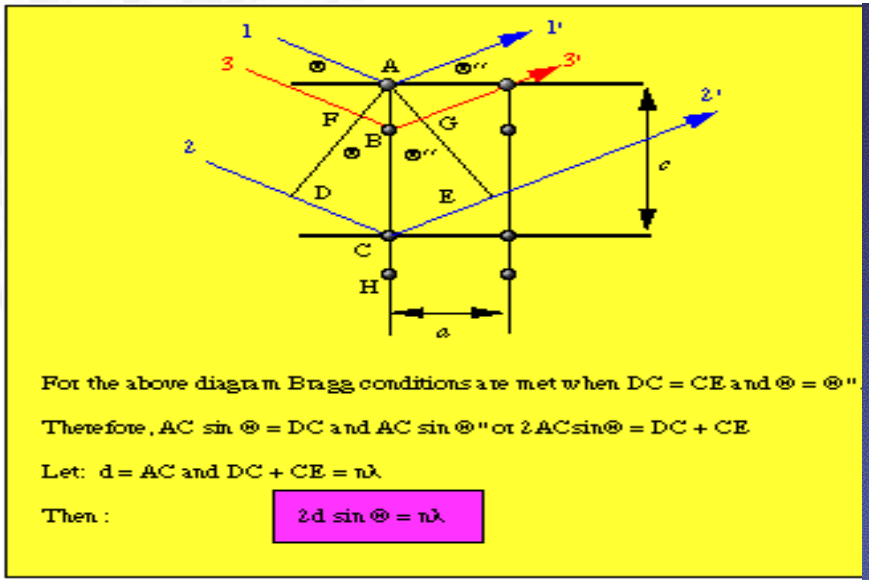

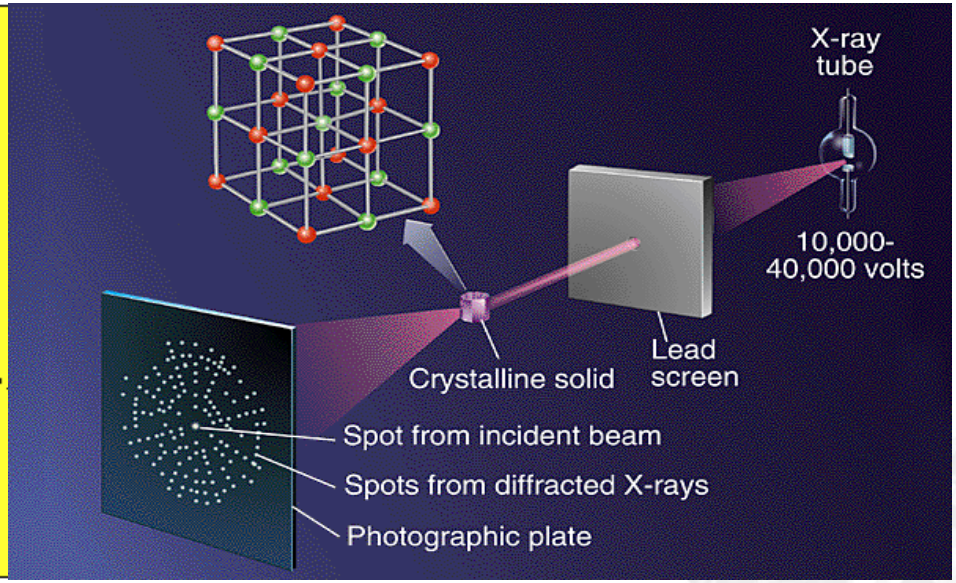

The atomic scale structure of crystals may be described on the basis of 3D periodic lattices in terms of a few parameters: Lattice type and symmetry
Unit cell parameters a, b, c, α, β, γ Atomic positions inside the unit cell: (x,y,z).

Diamond

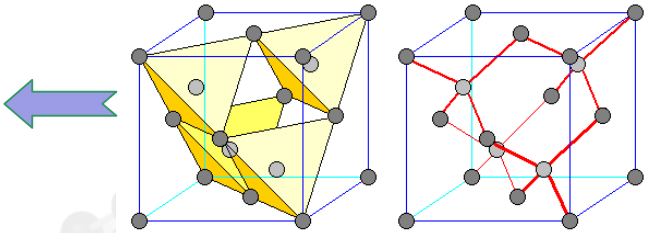

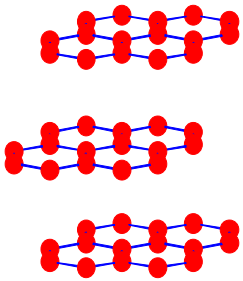

Graphite

These parameters/numbers allow to compute, understand and predict properties of crystals; also allow to "patent" crystalline pharmaceutical materials.

Example - Aspirin

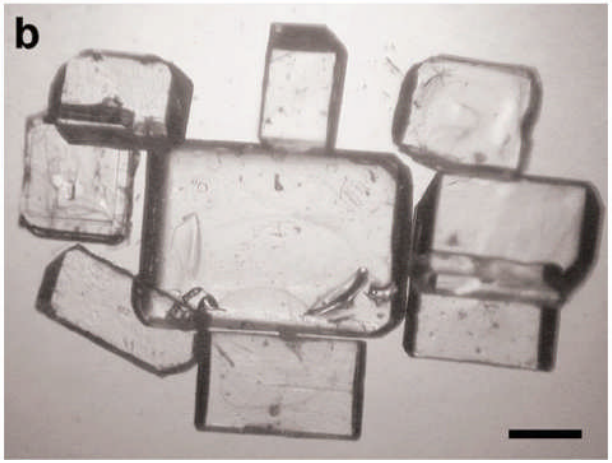

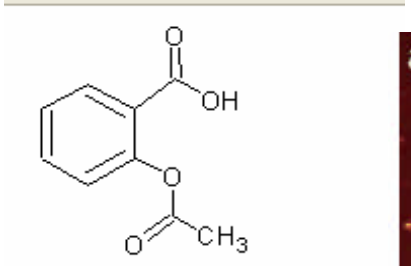

Aspirin

Acetylsalicylic Acid

$C_9H_8O_4$

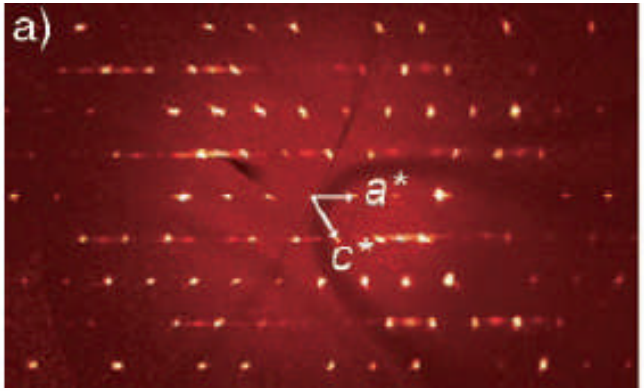

C.A. Medendorp et al. J. Pharm. Science **97** (2008) 1361.

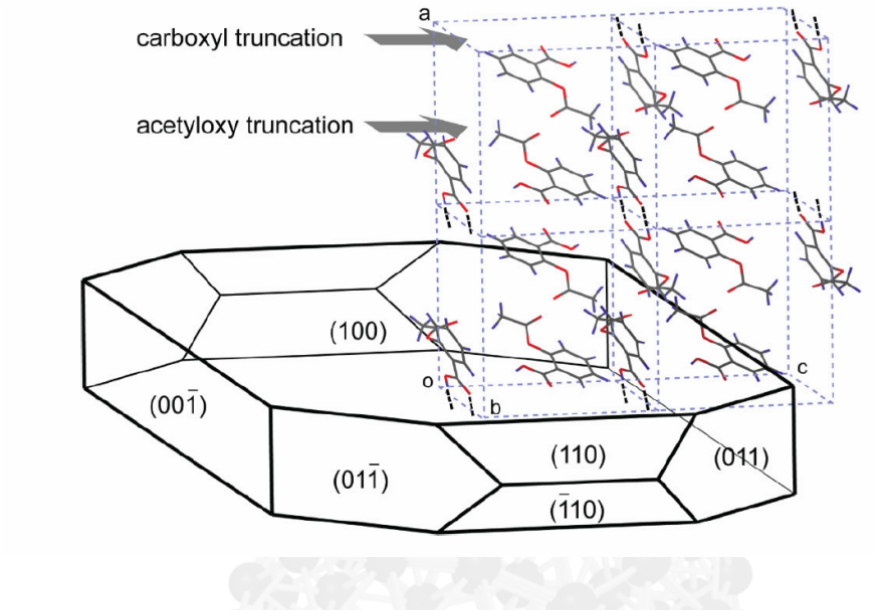

Aspirin crystals evaluated by single XRD indicated the crystals were of the monoclinic space group $P2_1/c$ with $a = 11.242(7)$, $b = 6.539(4)$, $c = 11.245(9)$ Å, and $\beta = 95.9(3)^\circ$. These values are

	x	y	
O4	14034(1)	7206(3)	5342(1)
O3	10104(1)	6881(2)	5965(1)
O2	11206(1)	6403(2)	4495(1)
O1	12855(1)	9117(2)	4122(1)
C1	13971(2)	6632(4)	3272(2)
C8	12605(2)	13029(3)	6337(2)
C7	11704(2)	12312(3)	6934(2)
C9	12984(2)	11944(3)	5417(2)
C2	13657(2)	7610(3)	4361(2)
C6	11170(2)	10505(3)	6598(2)
C5	10903(2)	7431(3)	5374(2)
C3	12459(2)	10119(3)	5094(2)
C4	11535(2)	9355(3)	5674(2)

Non-crystalline materials: glasses, polymers, composites..

Example: again carbon but "amorphous", i.e. coal.

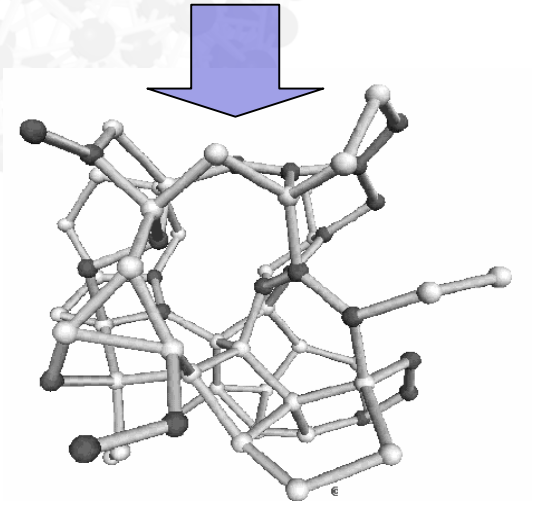

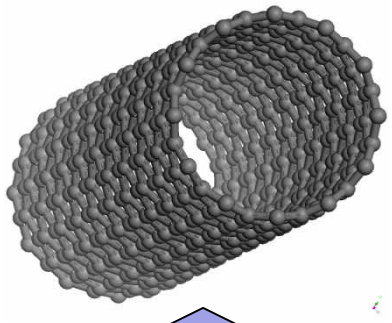

Example: again carbon but "nanotube"..

Atoms in non-crystals do not sit on the vertices of 3D periodic lattices.
Such materials are called "structurally disordered" yet they have a very well defined local (short + often intermediate) atomic ordering.
Why ? Nature of chemical bonding does not change (usually) between crystalline and amorphous state (e.g. quartz – silica glass)
We still need structure models parameters/numbers to describe this ordering.

Could we use x-rays ?

Experimental situation we face:

Long-range (~mm), periodic order | **Limited (~ nm) but measurable order** | **Short-range (sub-nano) order only**

Crystals | "Nanomaterials" | Non-crystals

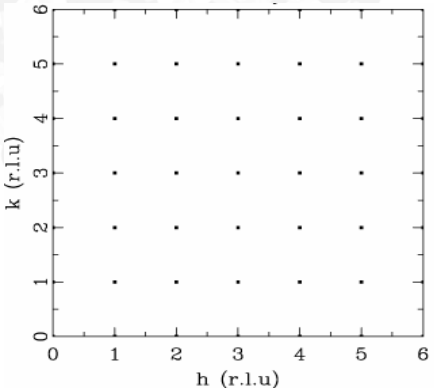

Simulated 2d patterns

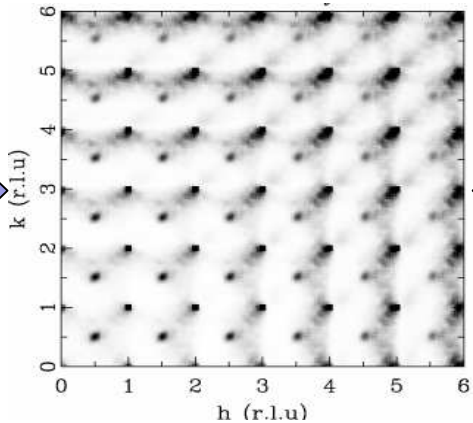

Simulated 2d patterns

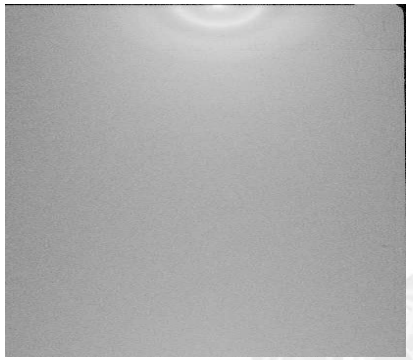

Bragg peaks only

Both Bragg peaks and diffuse scattering

Diffuse scattering only

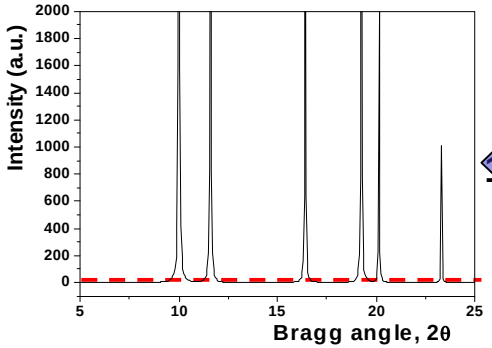

1d patterns

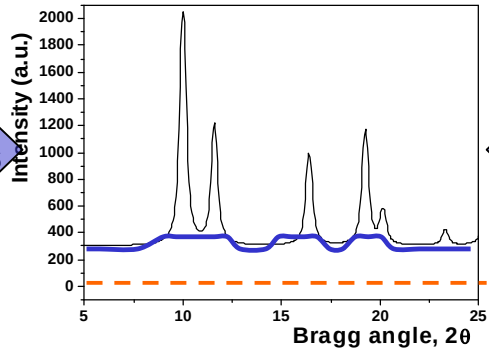

1d patterns

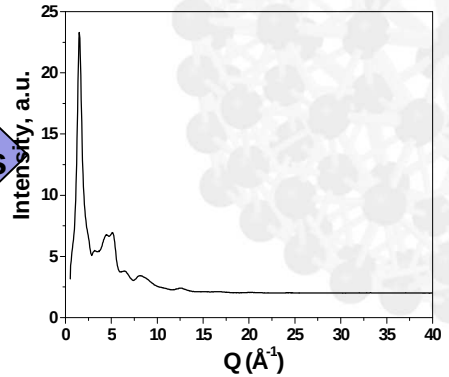

Diffraction patterns of "crystals" show many well-defined Bragg peaks.
Diffraction patterns of "glasses" show diffuse scattering only.
Diffraction patterns of "crystals with disorder", "nanoparticles", "composites" etc. may show both Bragg-like peaks (usually not so many and not so sharp) and diffuse scattering (that may not be neglected…)

What can be done ? Total XRD = High-energy XRD and real-space data analysis

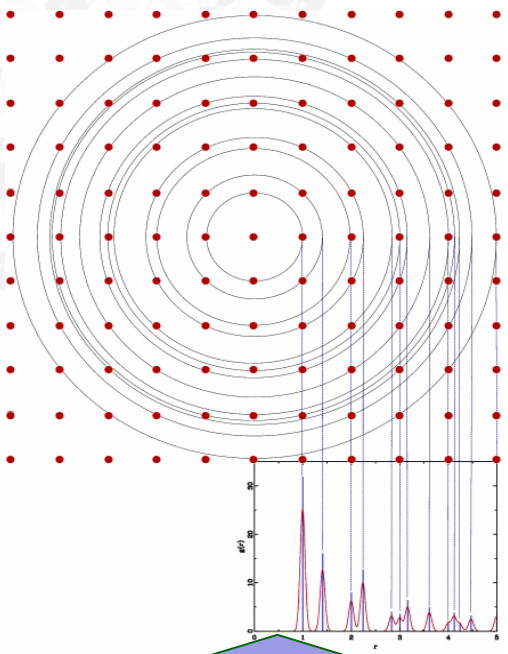

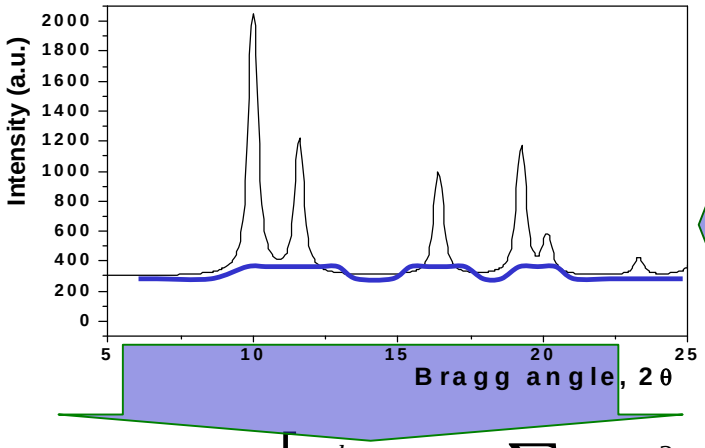

Diffraction experiment

$$S(Q) = 1 + \left[I^{el.}(Q) - \sum c_i f_i^2(Q) \right] / \left[\sum c_i f_i(Q) \right]^2$$

$$G(r) = (2/\pi) \int_{Q=0}^{Q_{max}} Q\,[S(Q) - 1] \sin(Qr)\, dQ\,,$$

$G(r) = 4\pi r[\rho(r) - \rho_o]$
$\rho(r)$ is the local and
ρ_o the average atomic density

$Q = 4\pi \sin(\theta)/\lambda = 1.0135 \sin(\theta) E[\text{keV}]$

i) The **atomic PDF** peaks at characteristic interatomic distances **reflecting** the **3D structure** of materials. **No long-range order or periodicity implied, i.e. well suited for any material.**

ii) Total XRD, and its Fourier transform, the atomic PDF takes into account **both the Bragg-like peaks and the diffuse scattering component of the XRD data. Both carry structural information !**

What do we need ?

Need x-rays of higher energy – to reach higher Q

Need stronger flux & more efficient detectors – to measure the diffuse component of XRD patterns with good statistics

Q: Where is the PDF's definition coming from ?

A: See below (after Klug and Alexander..)

For a collection of N atoms..

$$I = Nf^2 \sum_m \frac{\sin Sr_{mn}}{Sr_{mn}}$$

$$I = Nf^2 \left(1 + \sum_{m'} \frac{\sin Sr_{mn}}{Sr_{mn}}\right),$$

$$I = Nf^2 \left[1 + \int_0^\infty 4\pi r^2 \rho(r) \frac{\sin Sr}{Sr}\, dr\right].$$

$$I = Nf^2 \left\{1 + \int_0^\infty 4\pi r^2 [\rho(r) - \rho_0] \frac{\sin Sr}{Sr}\, dr + \int_0^\infty 4\pi r^2 \rho_0 \frac{\sin Sr}{Sr}\, dr\right\}.$$

$$i(S) = \frac{I}{Nf^2} - 1$$

$$\frac{I}{Nf^2} - 1 = \int_0^\infty 4\pi r^2 [\rho(r) - \rho_0] \frac{\sin Sr}{Sr}\, dr.$$

$$r[\rho(r) - \rho_0] = \frac{1}{2\pi^2} \int_0^\infty Si(S) \sin rS\, dS,$$

Here s= $Q=4\pi\sin(\theta)/\lambda=1.0135\sin(\theta)E[keV]$

For a multicomponent system s*i*(s) is "replaced" by F(Q) where:

$$F(Q) = Q \frac{I_a^{coh}(Q) - \langle f^2 \rangle}{\langle f \rangle^2}, \qquad (7)$$

where $\langle f^2 \rangle$ and $\langle f \rangle^2$ are short notations for $\langle f(Q) f^*(Q) \rangle$ and $\langle f(Q) \rangle \langle f^*(Q) \rangle$, respectively, and $I_a^{coh}(Q)$ is the coherent single-diffracted intensity per atom. I_a^{coh} and f^2 are expressed in dimensionless electron units. Note that I_a^{coh} does not contain contributions from multiple scattering, inelastic scattering or small-angle contributions arising from the finite size of the scattering volume.

Welcome to real space world: Si standard

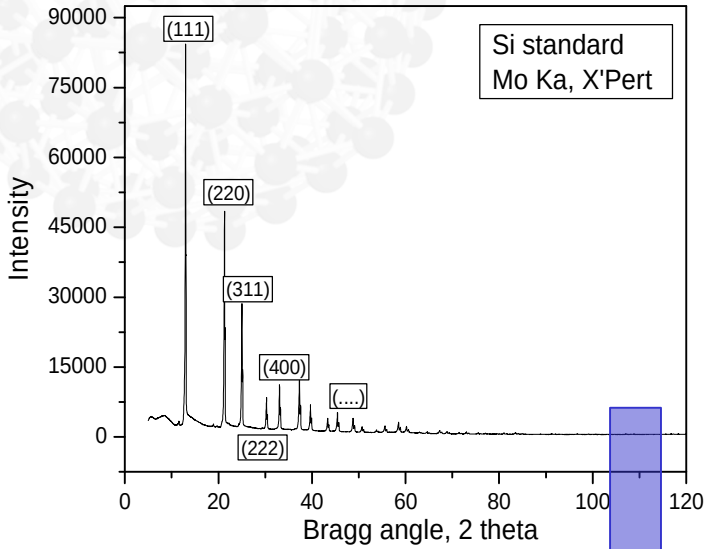

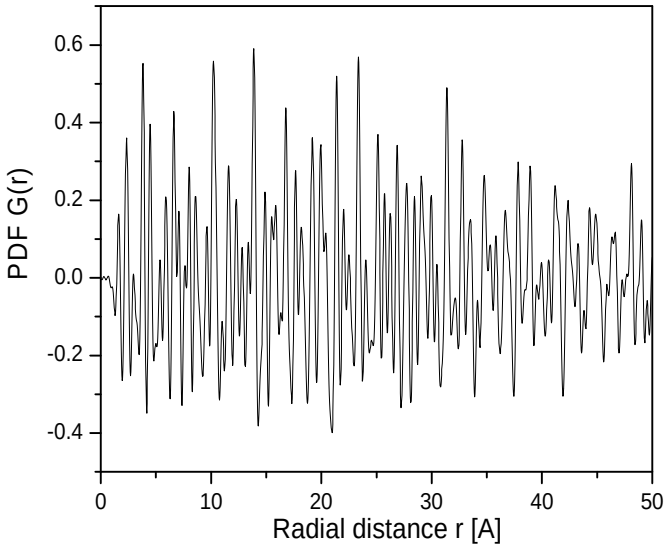

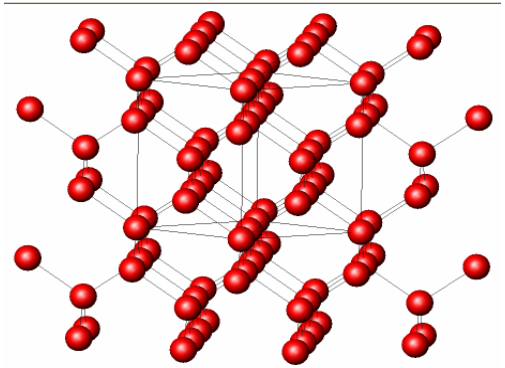

Si
S.G: F d 3 m (227)
Structure: diamond type
Cell parameters:
a=b=c=5.4309 A
α= β= γ= 90.0°
Si (8a) 0.125, …

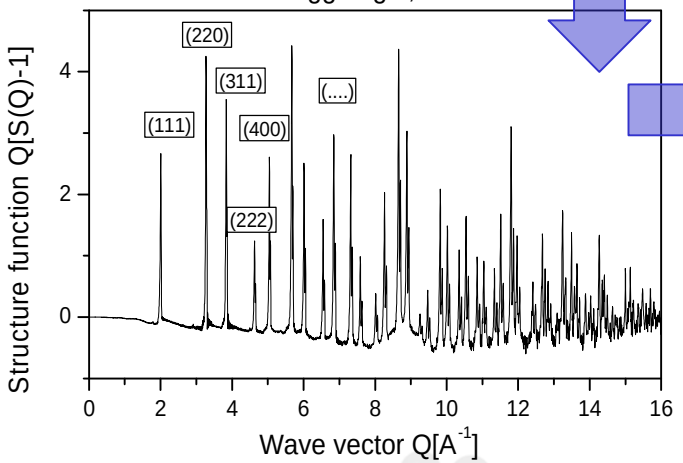

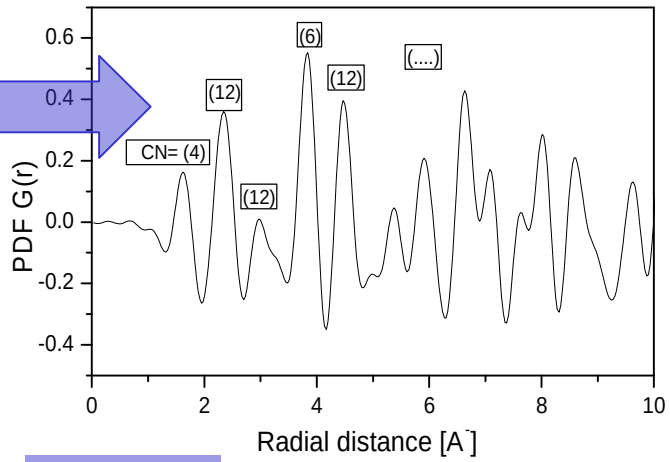

Reciprocal/diffraction space ← Fourier couple → Real space

$$S(Q)=1+\left[I^{el.}(Q)-\sum c_i f_i^2(Q)\right]/\left[\sum c_i f_i(Q)\right]^2 \longleftrightarrow G(r)=(2/\pi)\int_{O=o}^{Q_{max}} Q[S(Q)-1]\sin(Qr)dQ,$$

Back to pharmaceuticals: Aspirin

E = 80.7 keV, λ=0.1534 Å
1-ID, APS

$P2_1/c$

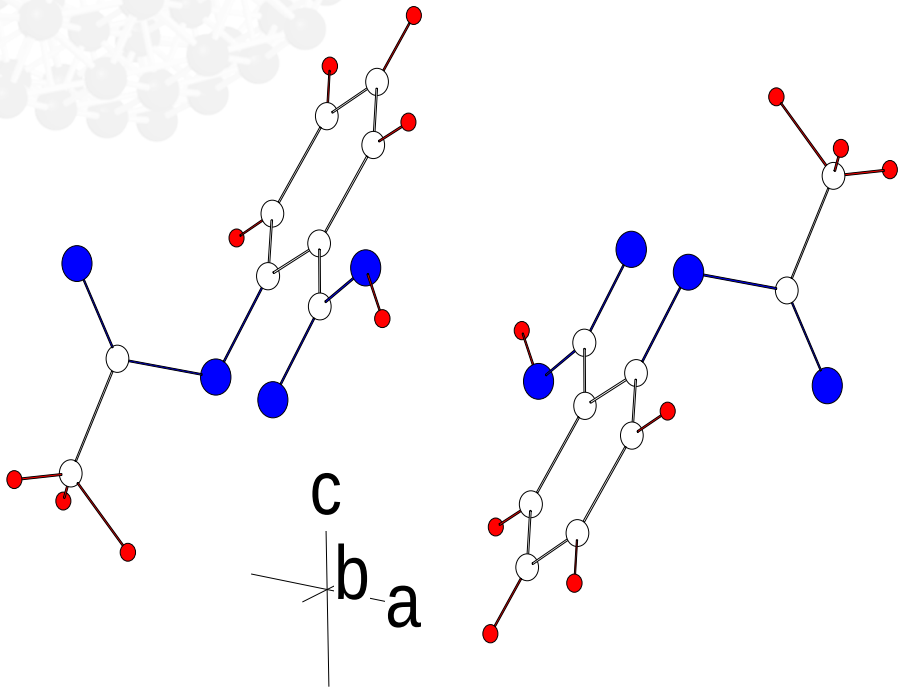

reciprocal space

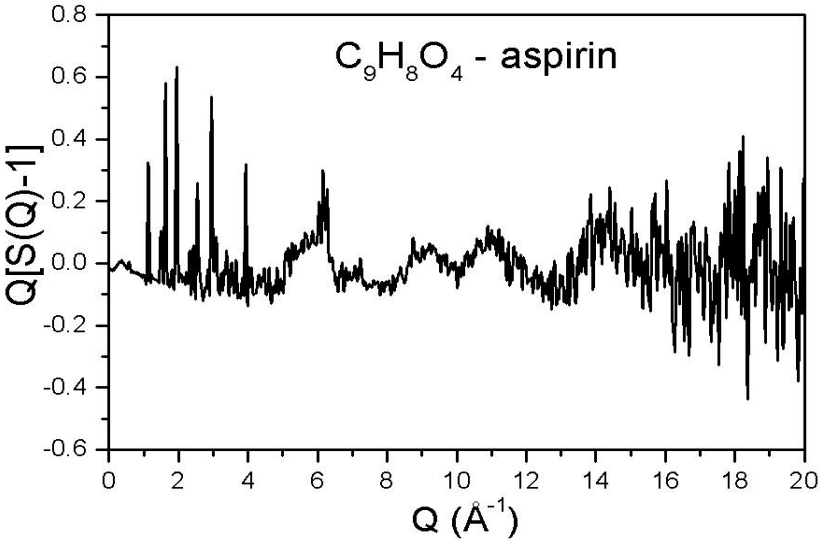

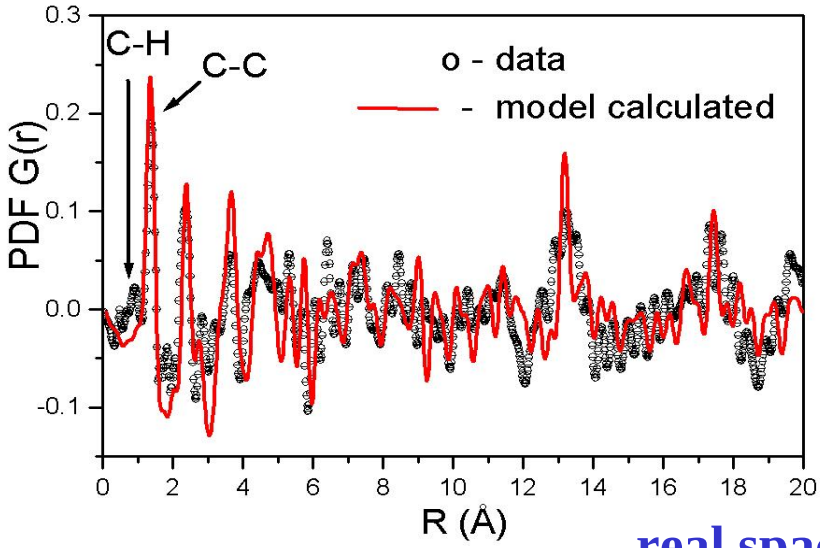

real space

Structural parameters: a list of {R_i ,CN_i}

R_i – coordination radii

CN_i – coordination numbers

A useful comparison: Traditional XRD/Rietveld Analysis (reciprocal space)

Structural determination assuming perfect 3D atomic ordering. Crystalline materials

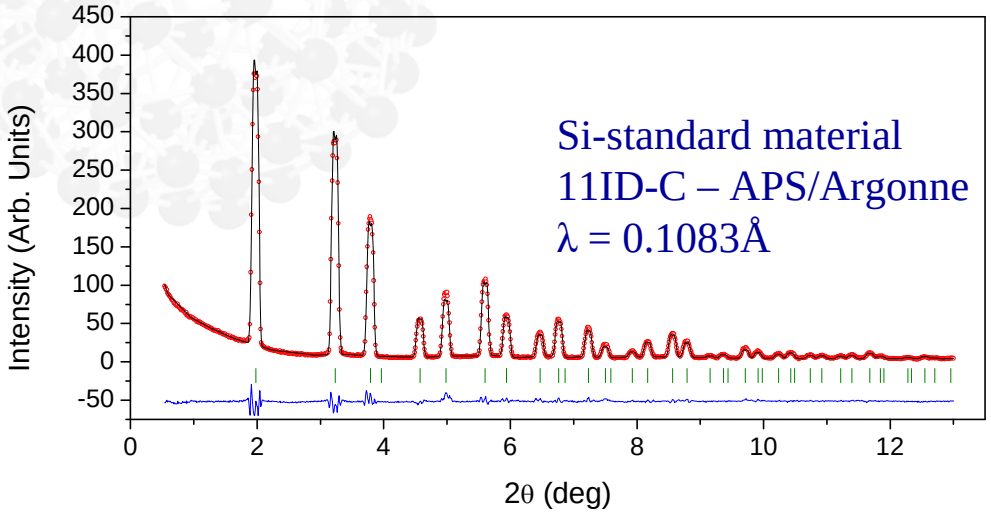

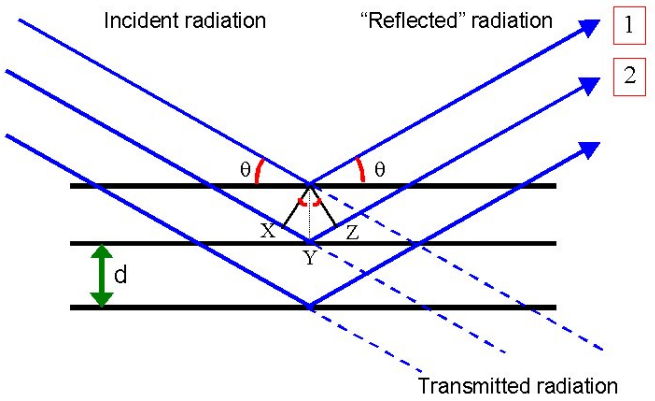

Bragg's Law: $2d\sin\theta = n\lambda$

Crystalline materials produce well defined Bragg peaks that can be used to solve the average, long-range structure of material. Bragg peaks come from a stack of regular atomic planes (Miller indexes) !

Bragg peaks → Unit cell → Indexing → Extinctions → Space group → Structural model → Rietveld refinement → Interatomic Distances, angles

Pair Distribution Function Analysis (real space)

High-resolution G(r) can be obtained by collecting diffraction data in wide *Q*-ranges ⇨ High-energy x-rays.

Structure refinement using PDF

Si-standard material
11ID-C – APS/Argonne
$\lambda = 0.1083$Å, $Q_{max} = 25$Å^{-1}

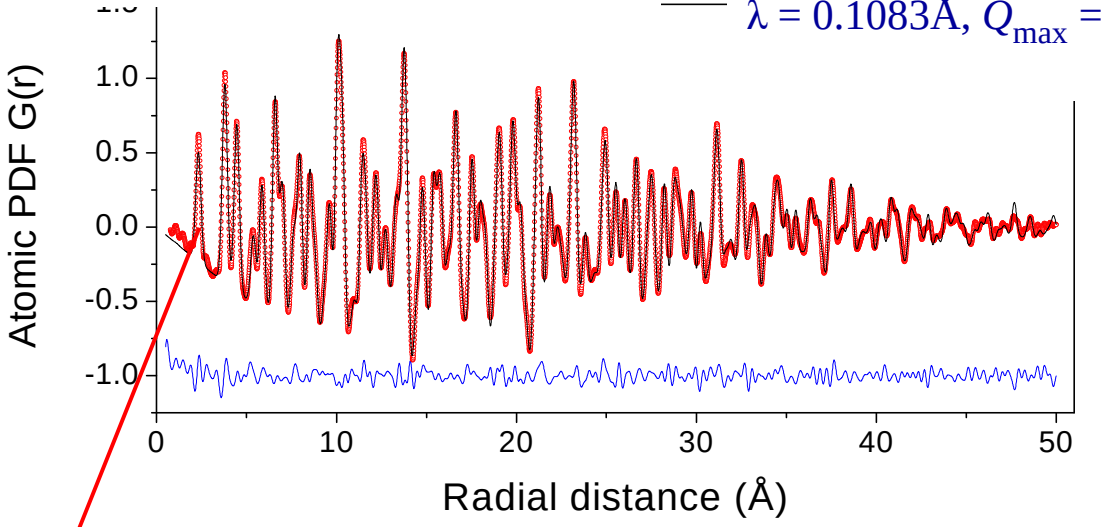

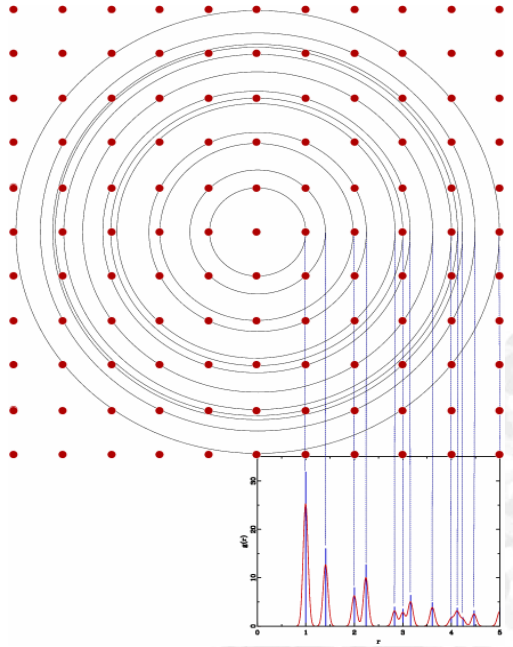

PDFs peaks reflect frequently occurring atomic pairs/coordination distances/spheres and not atomic planes ! Any material has a particular/unique coordination spheres distribution.….may serve as a "structural fingerprint" !

PDF peaks = Interatomic distances → Structural model (search and refinement) → If necessary may compute the XRD pattern

However, traditional (reciprocal space) and PDF (real space) analyses have different sensitivity to the atomic ordering in materials.
Traditional – Long-range order and translational periodicity (Bragg peaks only)
PDF – Any atomic ordering, periodic or not….does not matter.

How it is done: In-house high-energy XRD/PDF Experiments

In-house set up

E (x-rays) ~

MoKa 17 keV/ lambda=0.71 A

Ag Ka 22 keV/lambda=0.55 A

Q_{max} ~ 16-20 A^{-1}

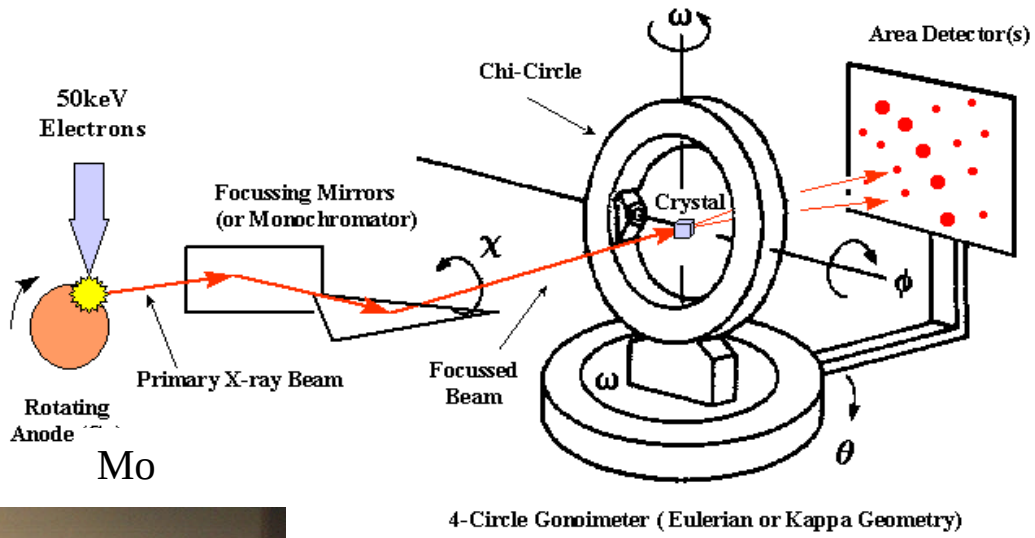

Mo

4-Circle Goniometer (Eulerian or Kappa Geometry)

CMU, Department of Physics

High-energy XRD/PDF experiments at synchrotrons

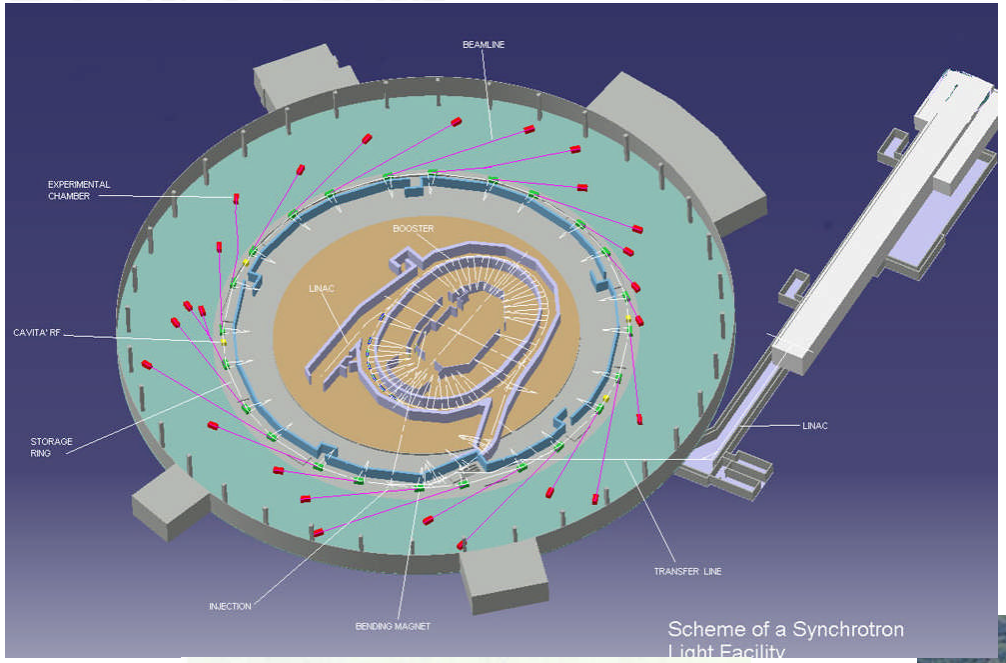

Scheme of a Synchrotron Light Facility

Synchrotron x-rays

Continuum of wavelengths

Energy range (0 ~ 150 keV vs 8 keV from Cu tube

(Advanced Photon Source, Argonne, Chicago)

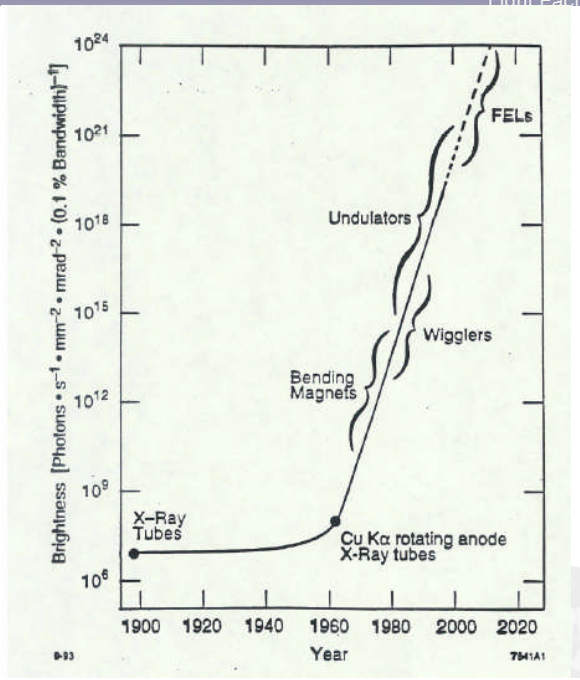

Example 1: Structure studies of cellulose by atomic PDFs

Cellulose is an organic compound with the formula $(C_6H_{10}O_5)_n$, a polysaccharide consisting of a linear chain of several hundred to over ten thousand β(1→4) linked D-glucose units.[2][3]

Cellulose is the structural component of the primary cell wall of green plants, many forms of algae and the oomycetes. Some species of bacteria secrete it to form biofilms. Cellulose is the most common organic compound on Earth. About 33 percent of all plant matter is cellulose (the cellulose content of cotton is 90 percent and that of wood is 50 percent).[4]

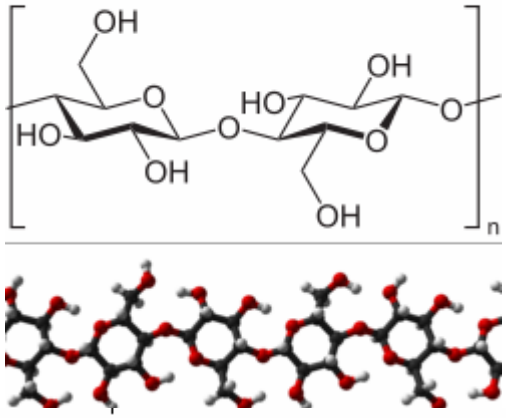

Several different crystalline structures of cellulose are known, corresponding to the location of hydrogen bonds between and within strands. Natural cellulose is cellulose I, with structures I_α and I_β. Cellulose produced by bacteria and algae is enriched in I_α while cellulose of higher plants consists mainly of I_β. Cellulose in regenerated cellulose fibers is cellulose II. The conversion of cellulose I to cellulose II is not reversible, suggesting that cellulose I is metastable and cellulose II is stable. With various chemical treatments it is possible to produce the structures cellulose III and cellulose IV.[12]

Commercial products [edit]

See also: dissolving pulp and pulp (paper)

Cellulose is the major constituent of paper, paperboard, and card stock and of textiles made from cotton, linen, and other plant fibers.

Cellulose can be converted into cellophane, a thin transparent film, and into rayon, an important fiber that has been used for textiles since the beginning of the 20th century. Both cellophane and rayon are known as "regenerated cellulose fibers"; they are identical to cellulose in chemical structure and are usually made from dissolving pulp via viscose. A more recent and environmentally friendly method to produce rayon is the Lyocell process.

Cellulose is the raw material in the manufacture of nitrocellulose (cellulose nitrate) which was historically used in smokeless gunpowder and as the base material for celluloid used for photographic and movie films until the mid 1930s.

Cellulose is used to make water-soluble adhesives and binders such as methyl cellulose and carboxymethyl cellulose which are used in wallpaper paste. Microcrystalline cellulose (E460i) and powdered cellulose (E460ii) are used as inactive fillers in tablets[9] and as thickeners and stabilizers in processed foods. Cellulose powder is for example used in Kraft Parmesean Cheese to prevent caking inside the tube.

Cellulose is used in the laboratory as the stationary phase for thin layer chromatography. Cellulose fibers are also used in liquid filtration, sometimes in combination with diatomaceous earth or other filtration media, to create a filter bed of inert material. Cellulose is further used to make hydrophilic and highly absorbent sponges.

Cellulose insulation made from recycled paper is becoming popular as an environmentally preferable material for building insulation. It can be treated with boric acid as a fire retardant.

Structure studies of cellulose by atomic PDFs

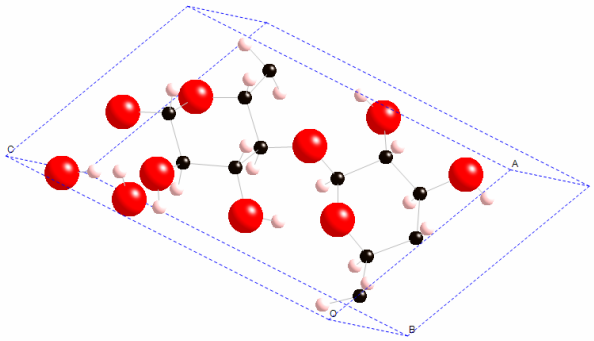

Cellulose Ia

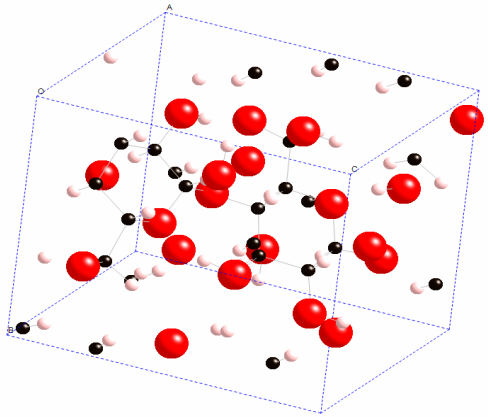

Cellulose Ib

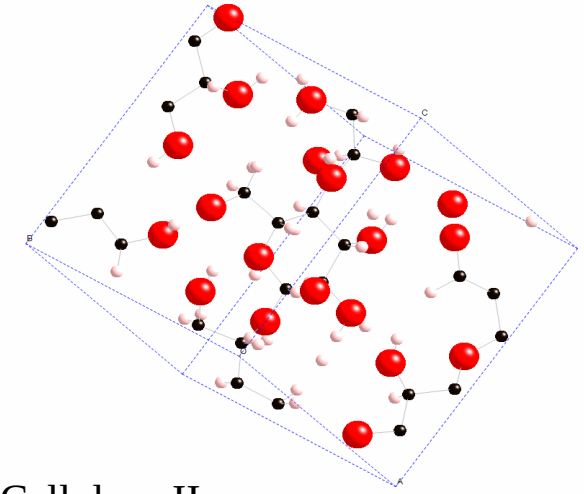

Cellulose II

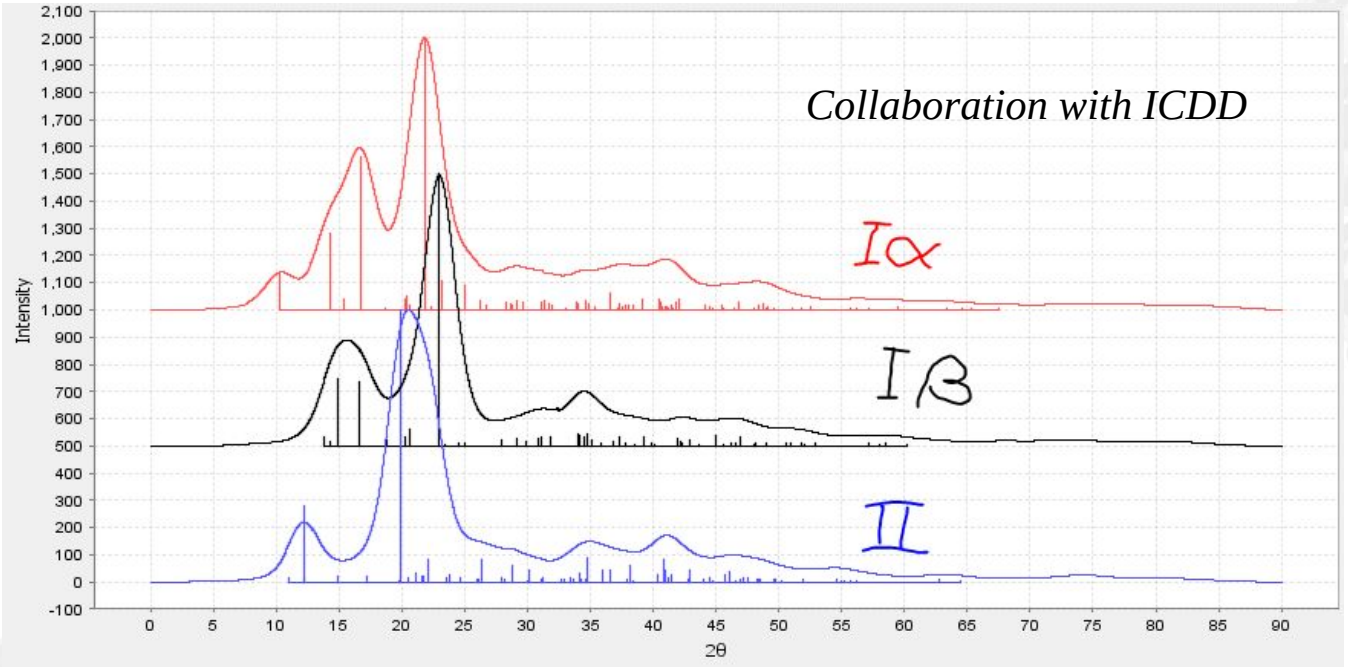

Traditional (Bragg) XRD patterns; Cu Ka radiation

Structure studies of cellulose by atomic PDFs

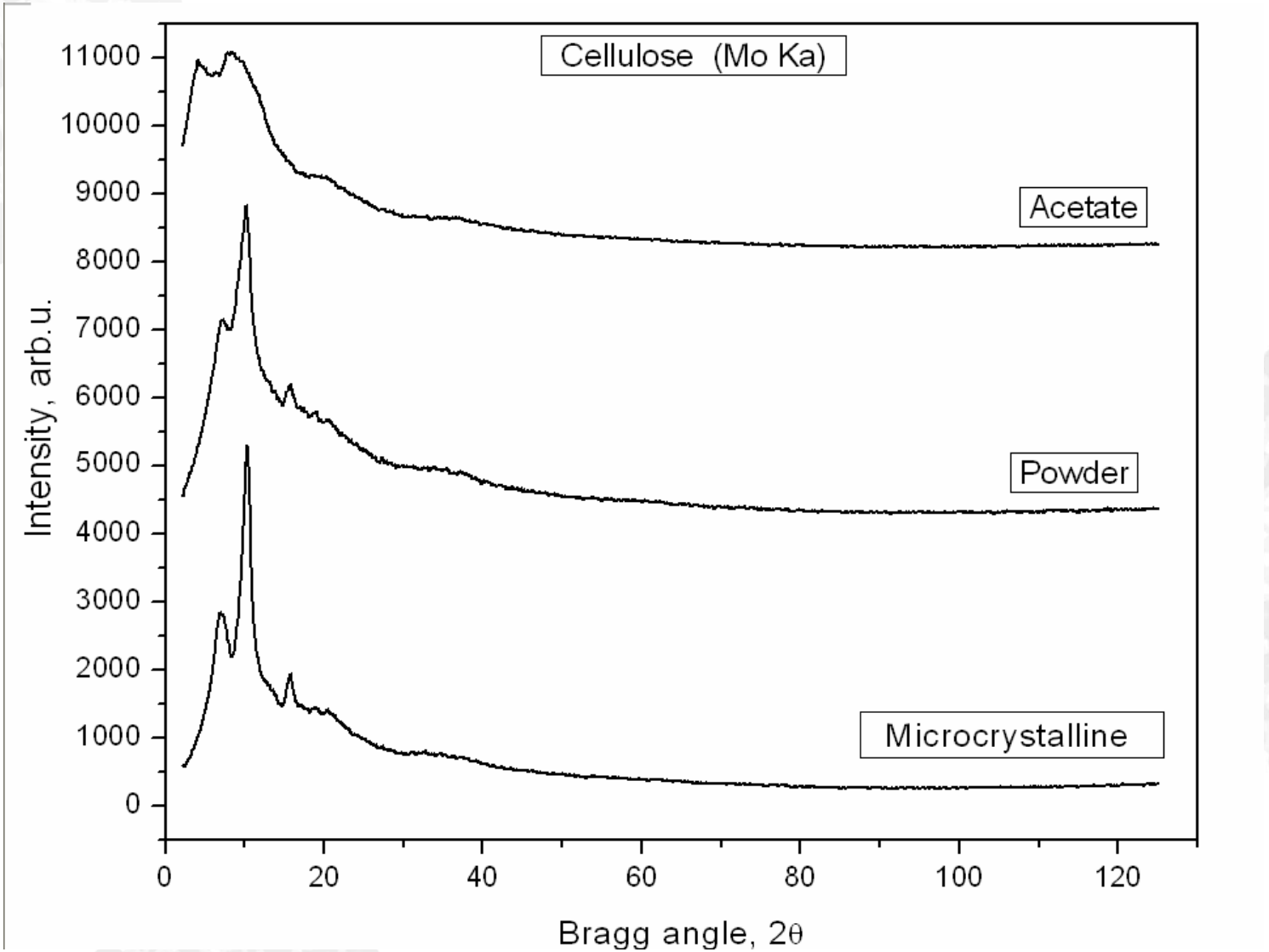

Traditional (Bragg) XRD patterns; Mo Ka radiation

Structure studies of cellulose by atomic PDFs

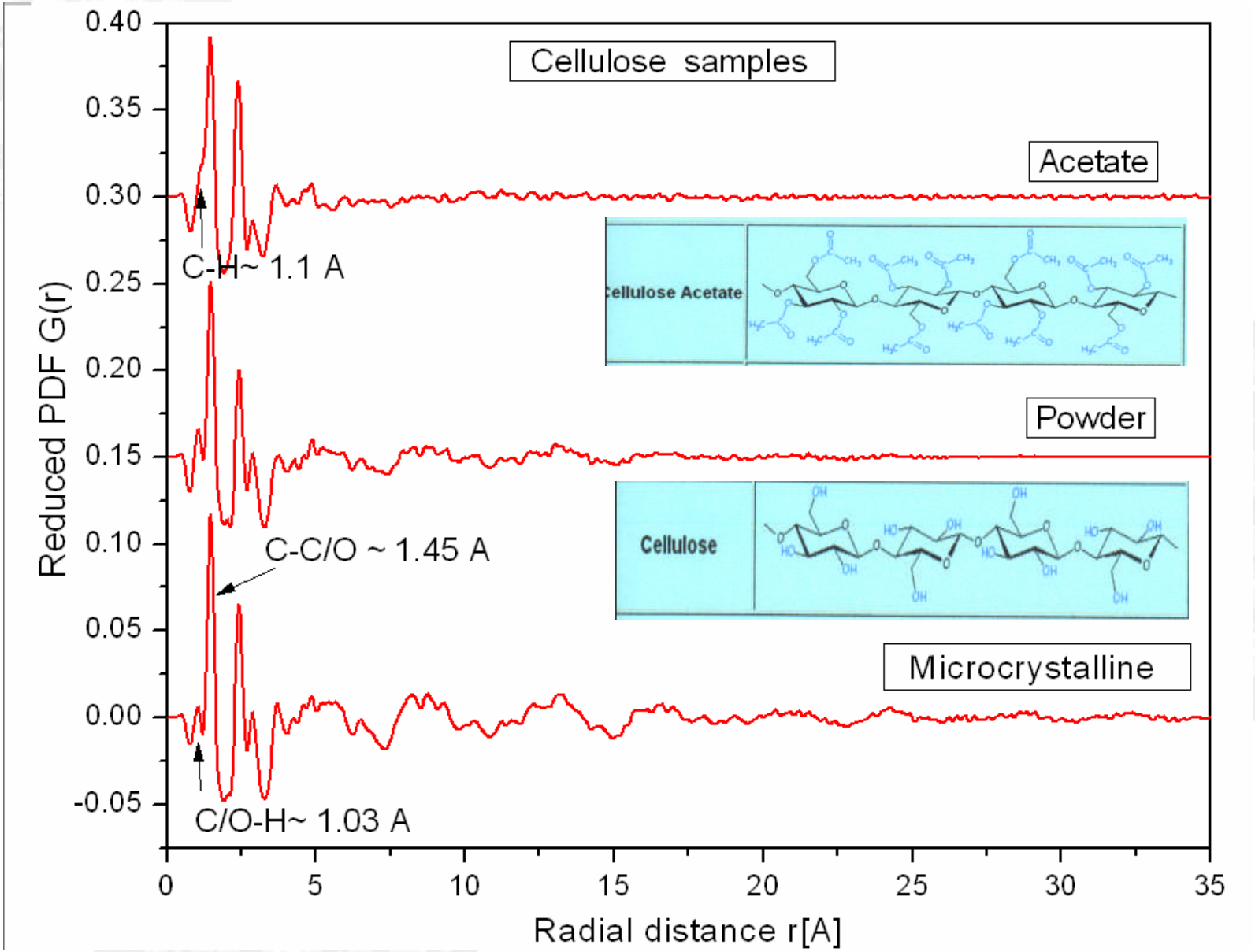

Atomic PDFs from synchrotron data

Structure studies of cellulose by atomic PDFs

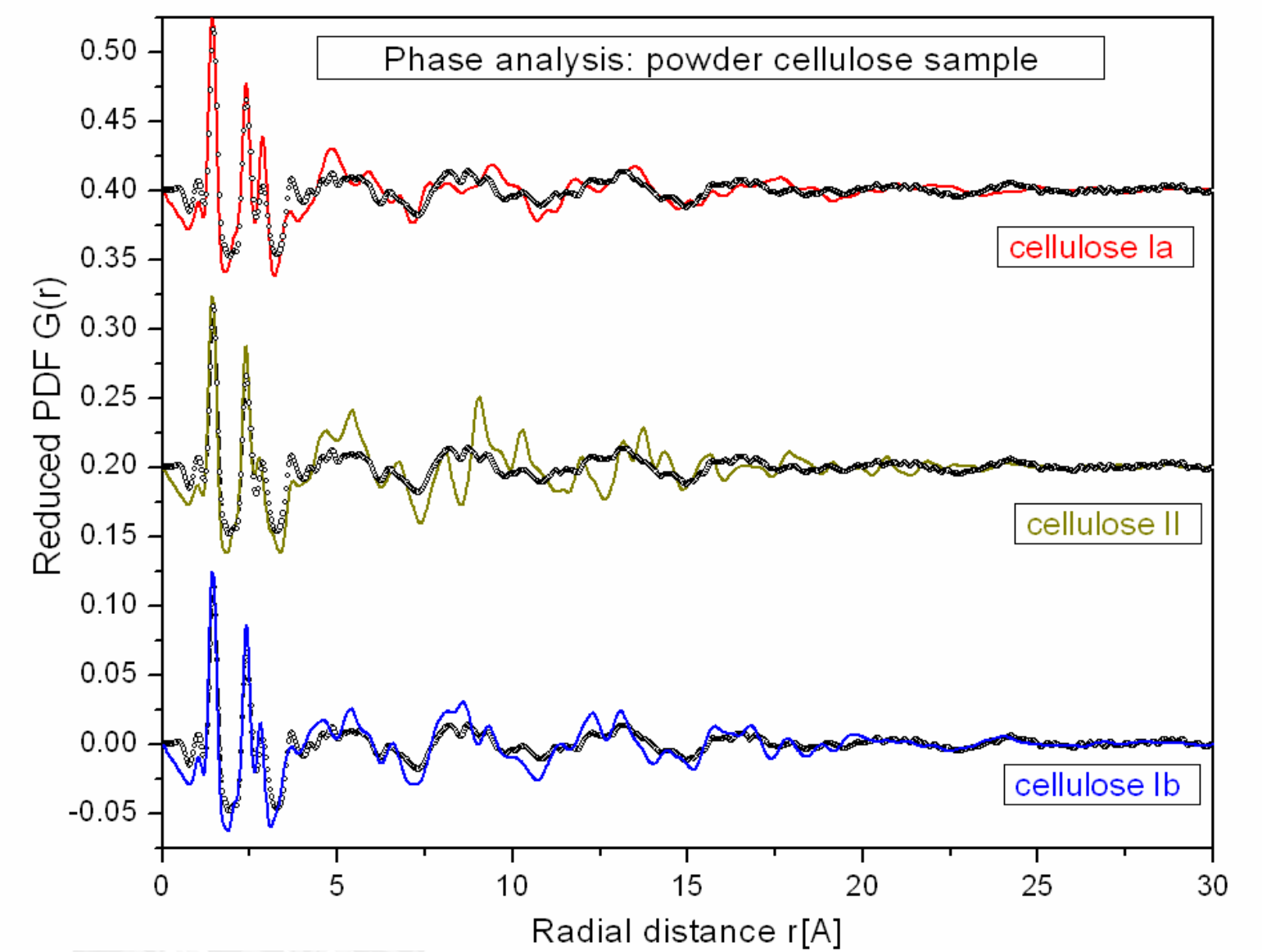

Example 2: Structure studies of other organic polymeric products…

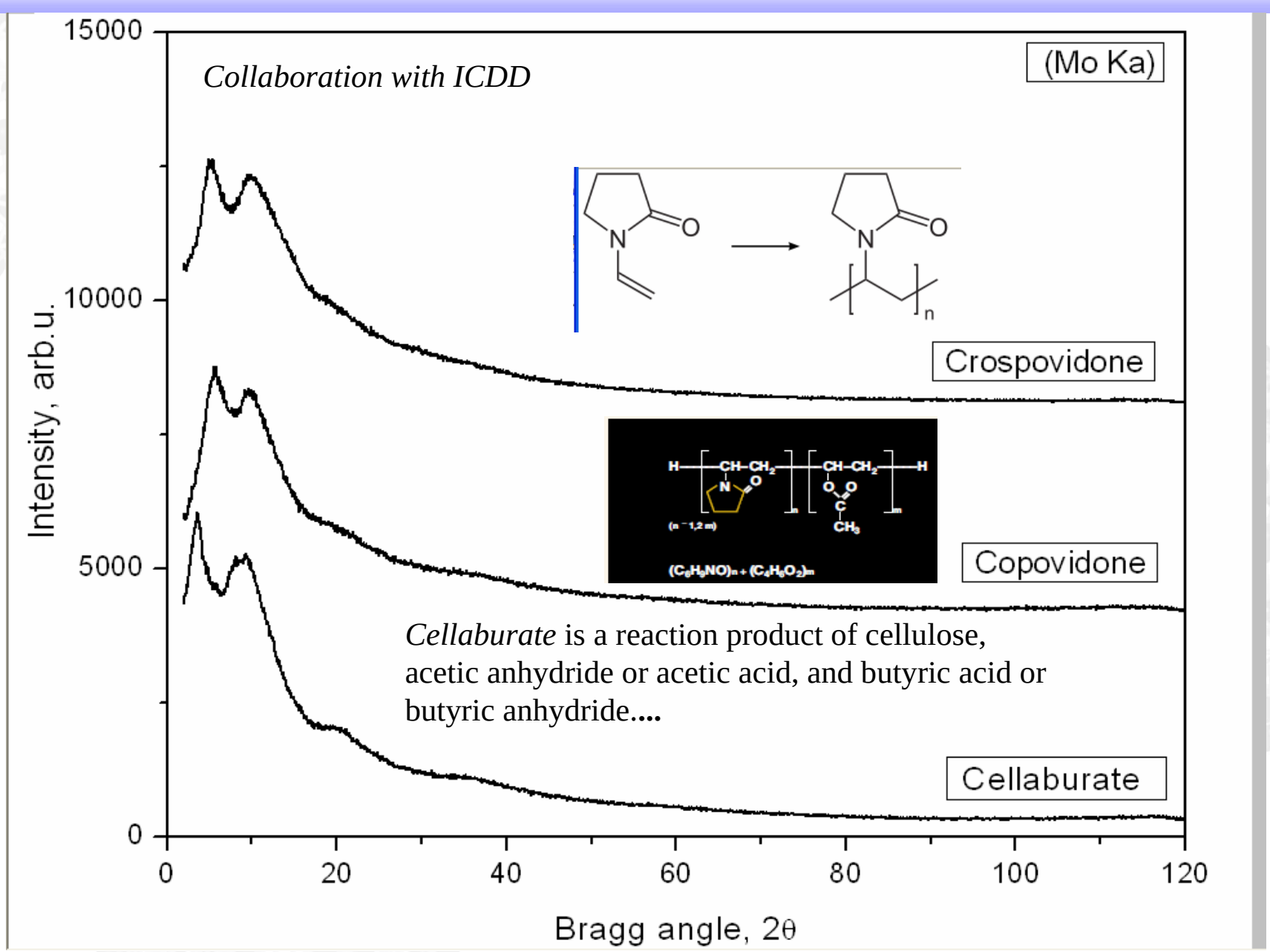

Structure studies of other organic polymeric products…

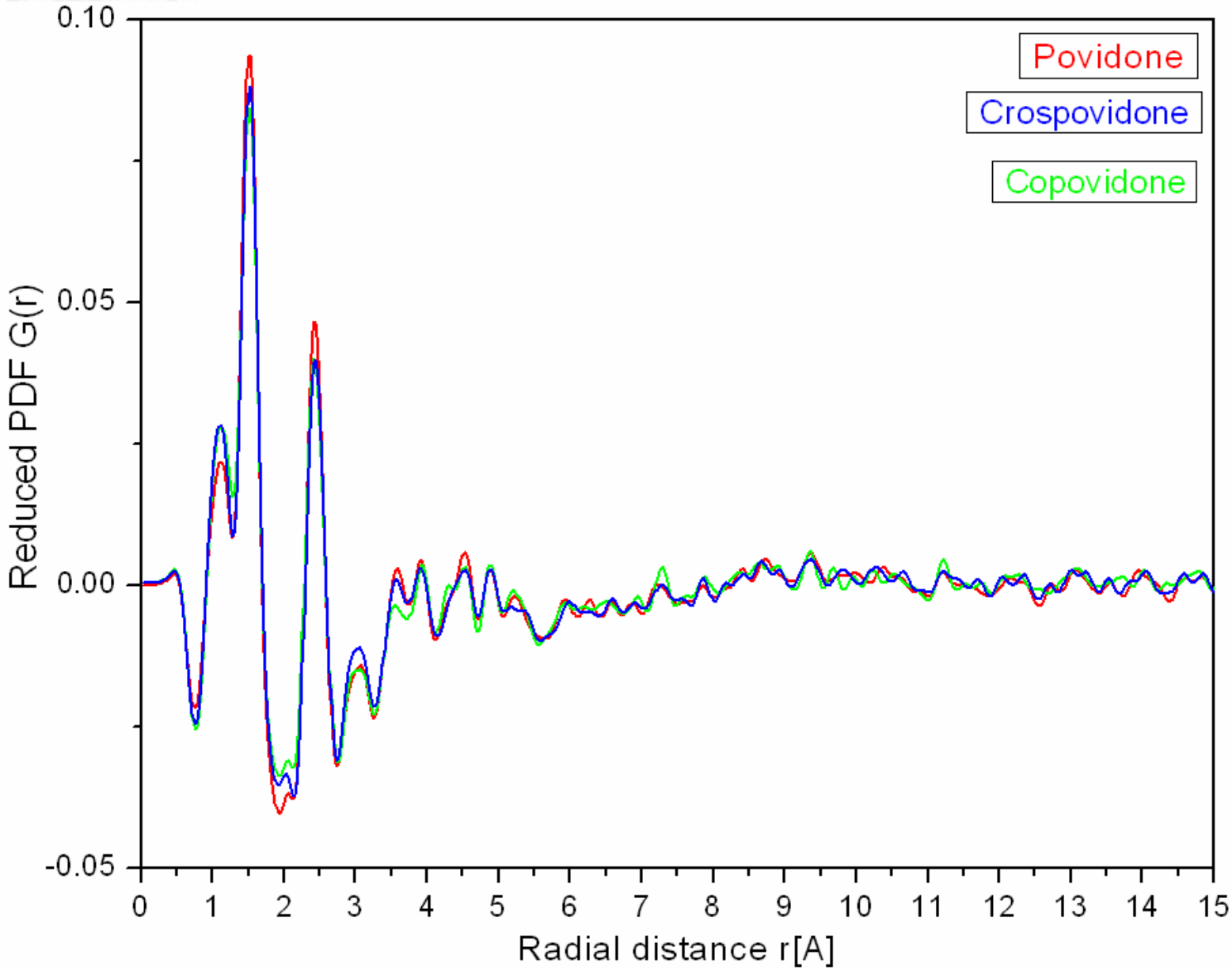

Atomic PDFs from synchrotron data

Example 3: Crystallization of lactose

Lactose

Chemical Formula:

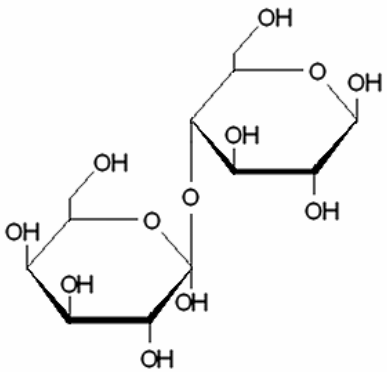

Synonyms

Milk Sugar

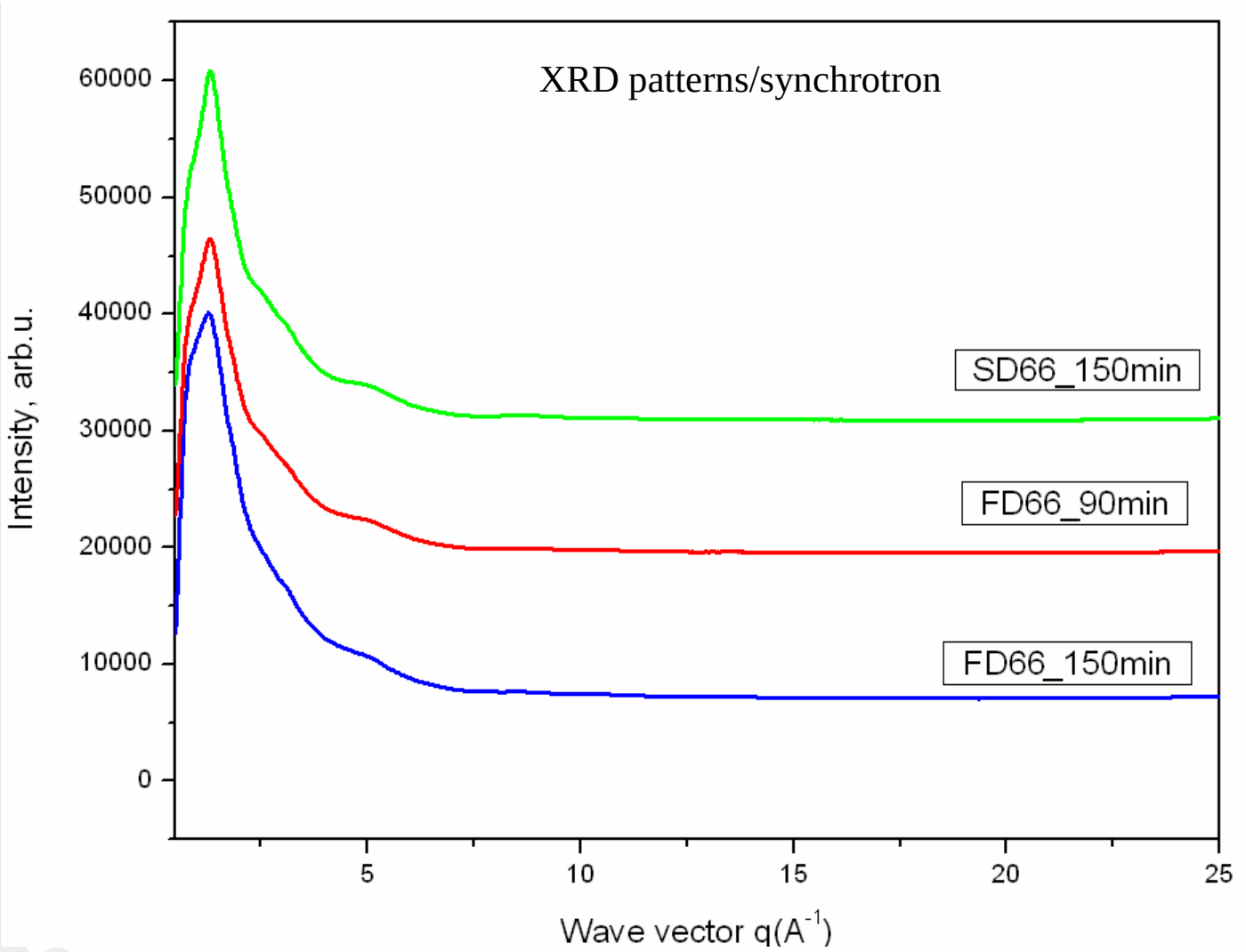

Sample dried at different conditions and crystallized for different times

Collaboration with Sandra Weiling, U. Bonn and Panalytical

Crystallization of lactose:

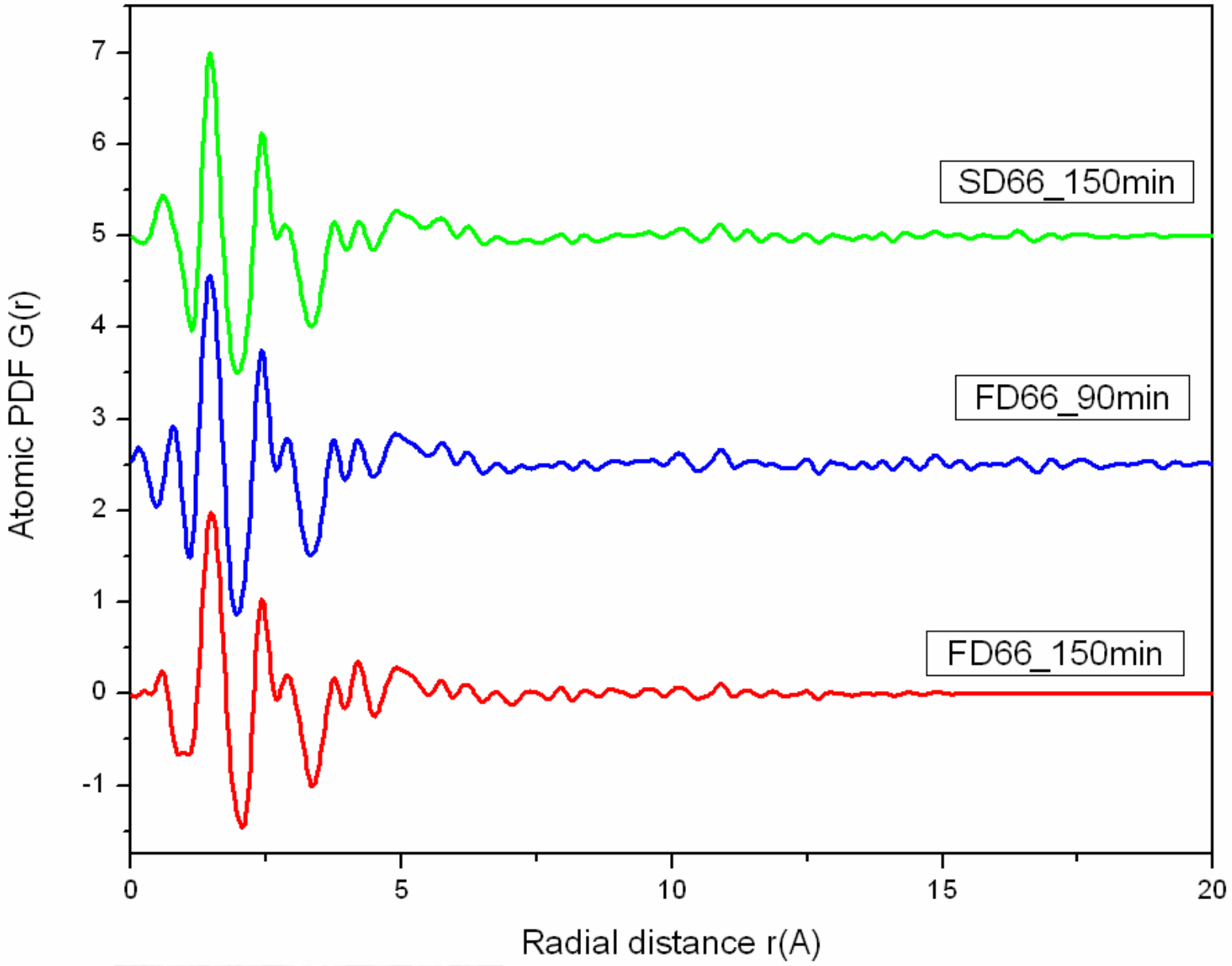

Atomic PDFs from synchrotron data

Example 4: Organic macromolecules for drug delivery

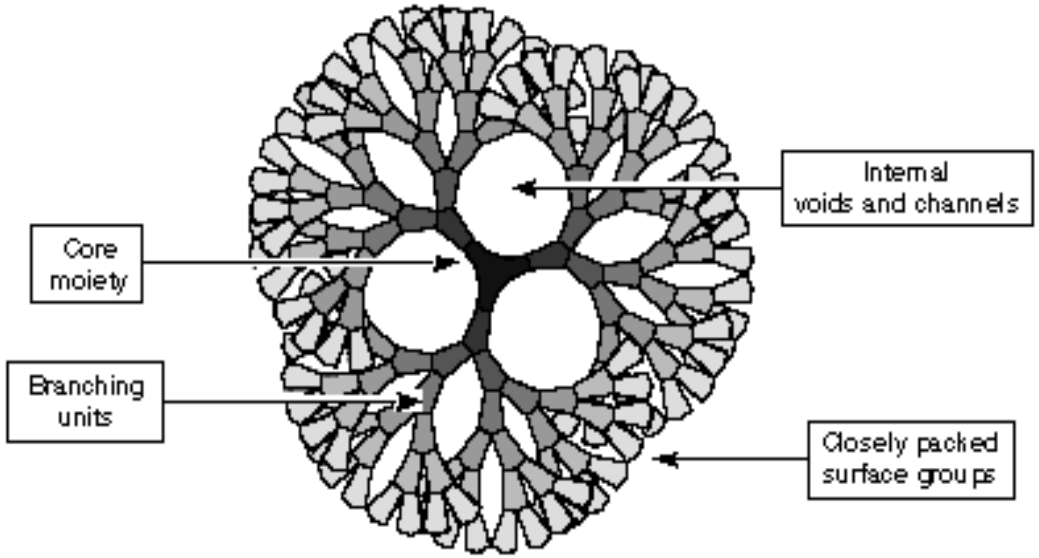

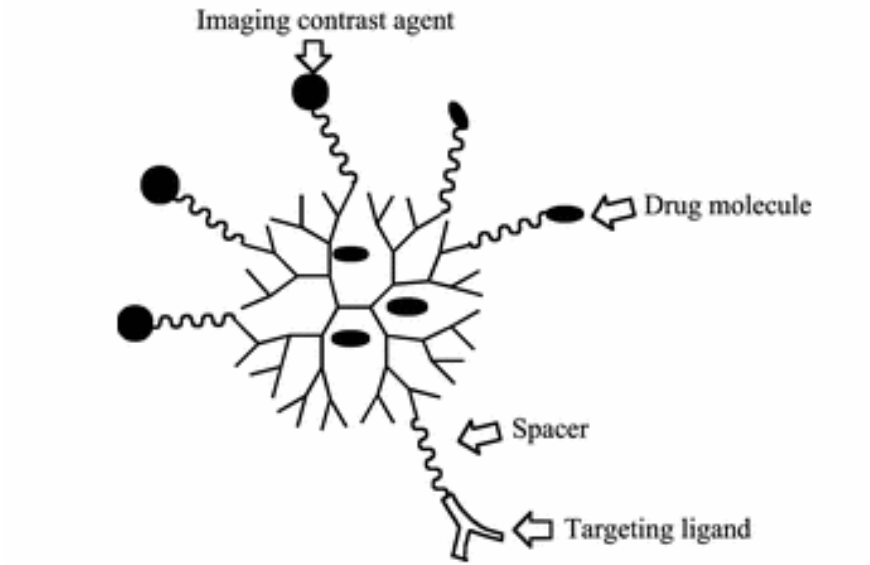

Collaboration with DNT

Dendrimers: consist of a series of chemical shells built on a small core molecule. Can be designed with a variety of organic and inorganic cores and branches, with tunable branch length, multiplicity and surface functionality:

Applications:

Polymer mimics of globular proteins
Building blocks of multifunctional nanocomposites
Hosts of guests molecules and nanoparticles

Questions: Is the interior hollow ?
How big is the free volume, if any ?

Organic macromolecules for drug delivery

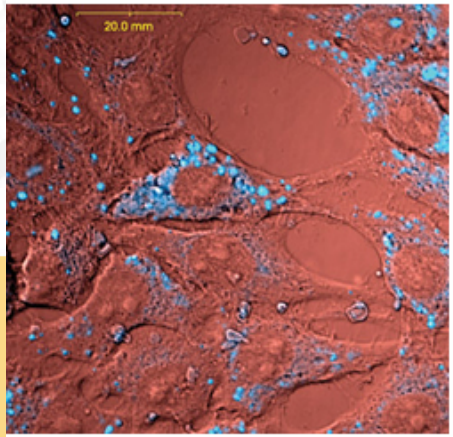

Nanocomposites taken up by human body cells exhibit blue fluorescence when subjected to UV excitation, as seen in this confocal microscope image. Exposure to IR radiation could allow their use in treatment as well. Courtesy of Lajos Balogh, Roswell Park Cancer Institute.

In cancer cells, bubbles began to appear at energies 100 times lower than in cells containing no nanocomposite particles. When small and nonlethal, the bubbles were easily recognizable in ultrasound images. Increasing laser power generated larger bubble that caused cell lysis. Bubbles disappeared before they could contact adjacent cells, however, and the radiation levels used did not harm cells that collected a few or no composites.

PAMAM dendrimers in more detail

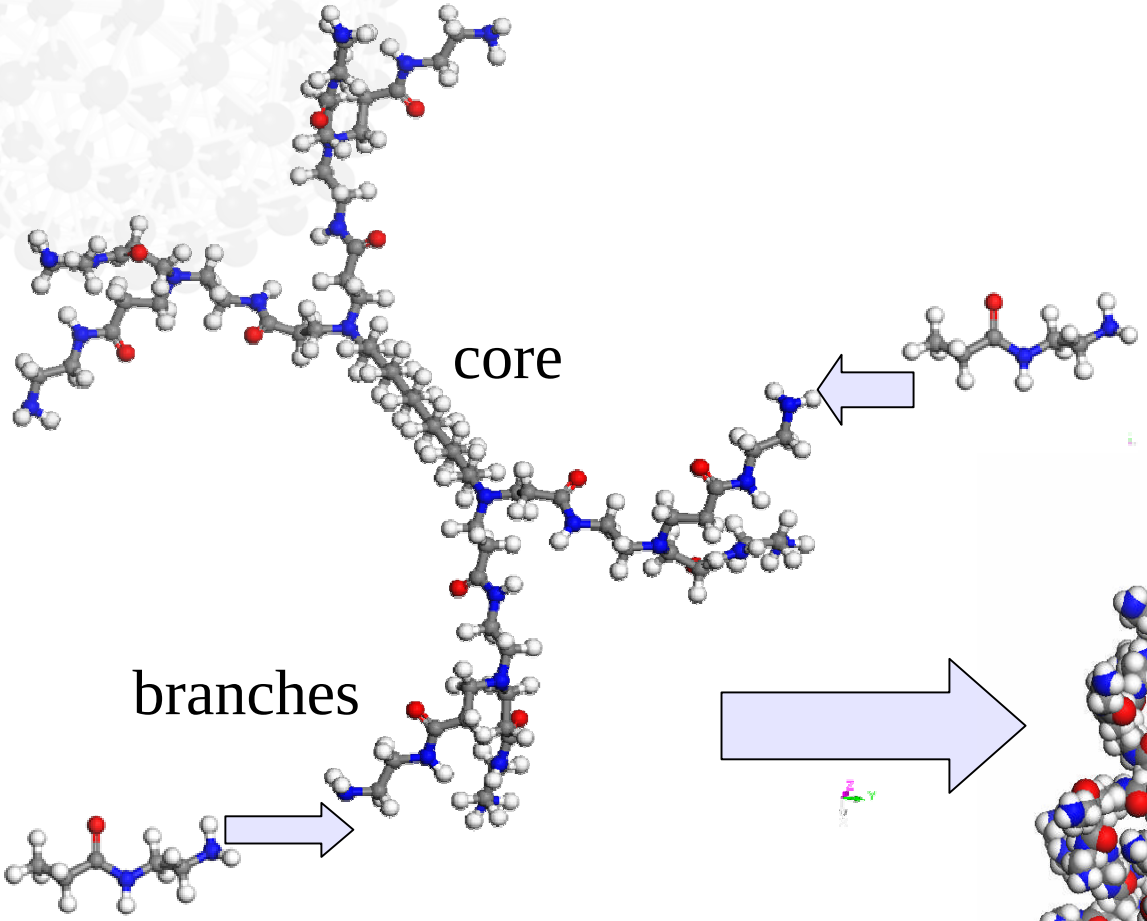

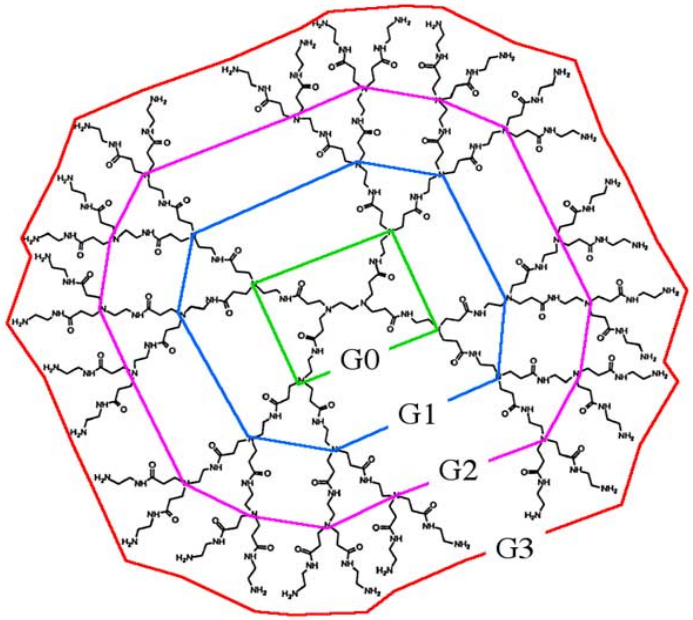

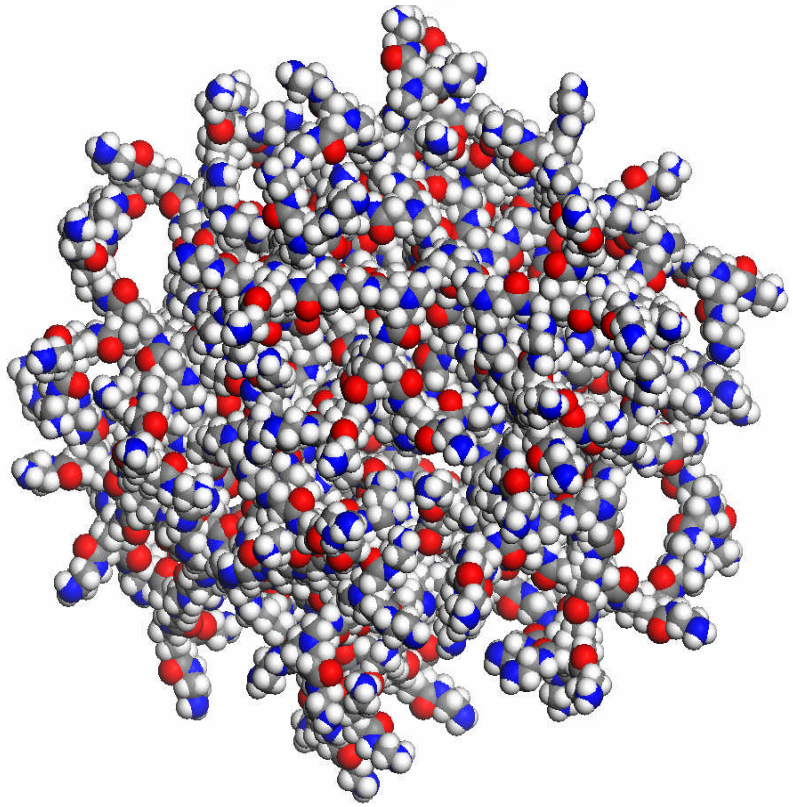

3D structure depends on the preparation technique employed (divergent/convergent,solvent), repetitive units, generation number etc.

Structure study of 7th generation PAMAM

Fullerene – 3D ordered lattice of rigid C60 molecules

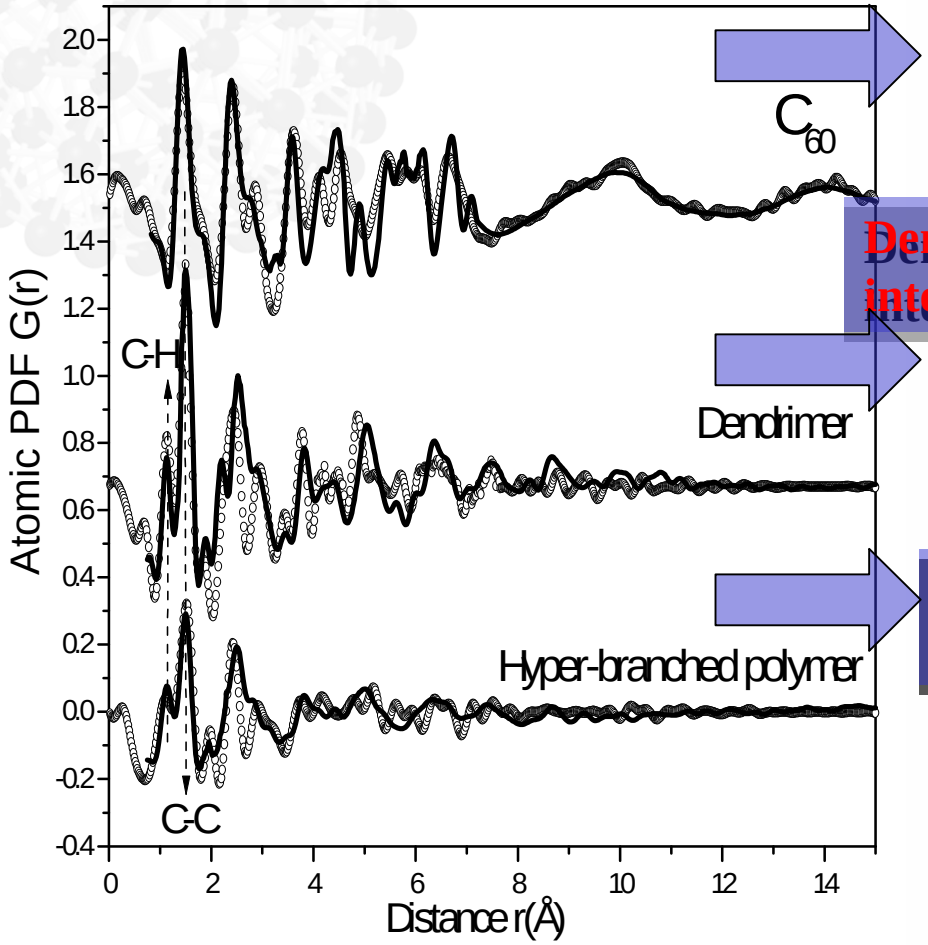

Experimental(dots) and model(line) atomic PDFs for fullerene, PAMAM dendrimers and hyper-branched polymers

Dendrimers = semi regular network with open interior narrow distribution of cavities

Hyper-branched: less regular but still open network; wide distribution of cavities

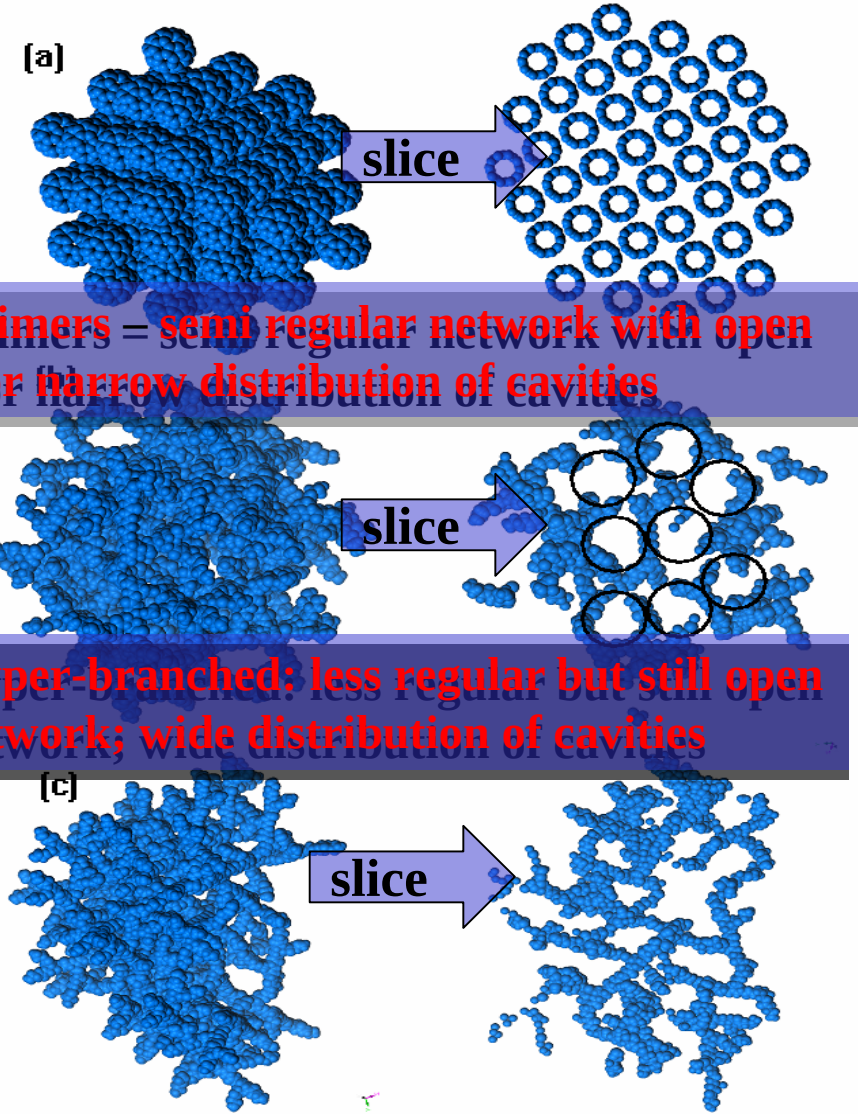

Fragments of structure models for fullerene, PAMAM dendrimers and hyper-branched polymers

PDF study of 7th generation PAMAM

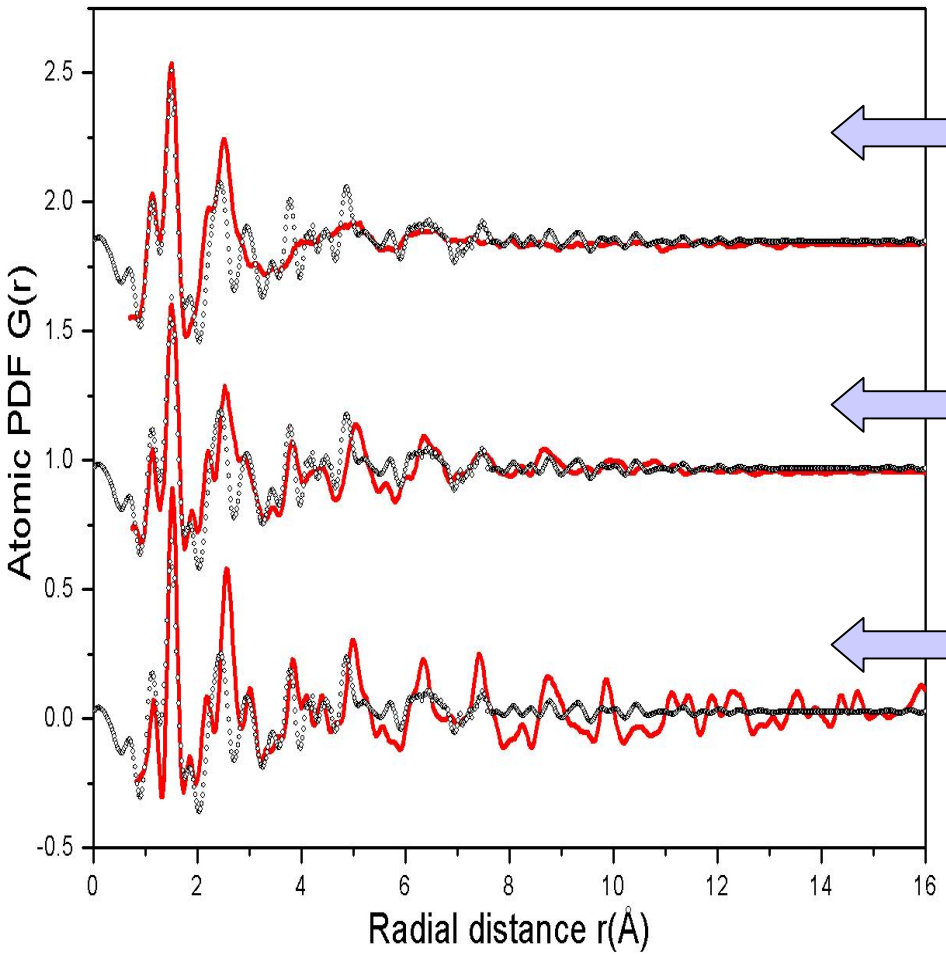

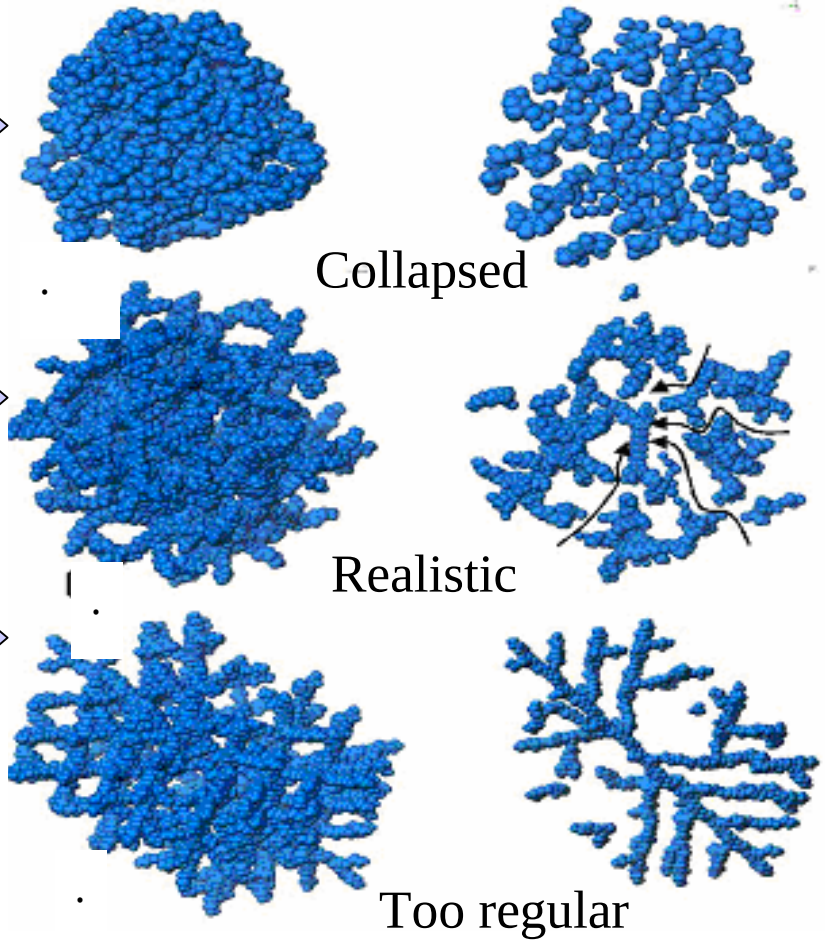

Exp. data – symbols
Model data – line in red

3D models of PAMAM dendrimers

PDF study of 7th generation PAMAM

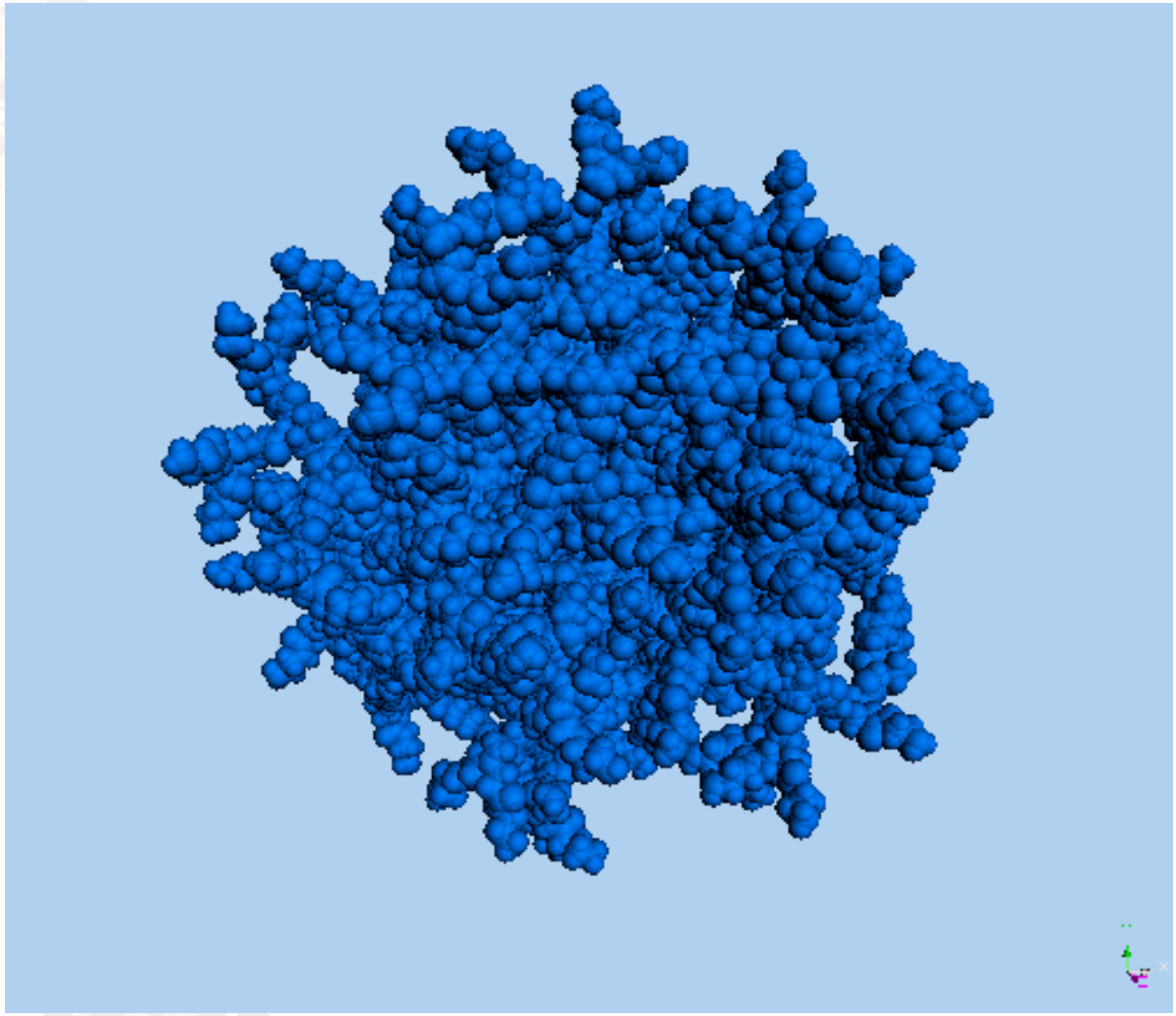

Example 5: Chemical specificity: PtPd nanoparticles in solution

Collaboration with R. Nuzzo, U. Illinois

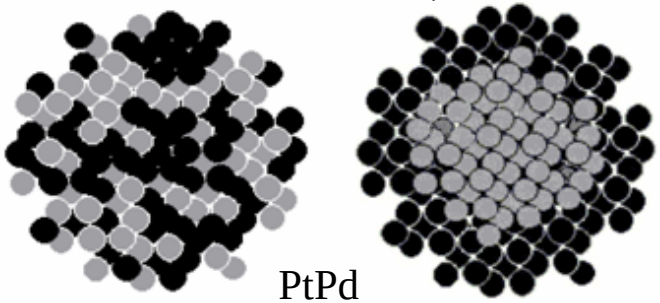

PtPd

Random alloy nanoparticle

Core-shell nanoparticle

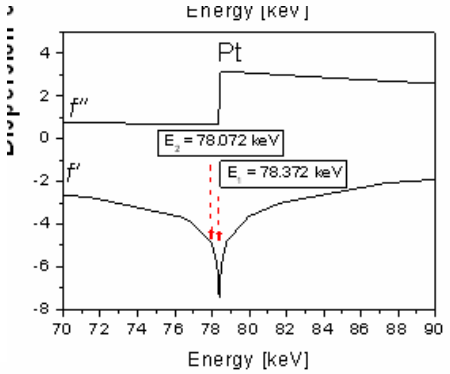

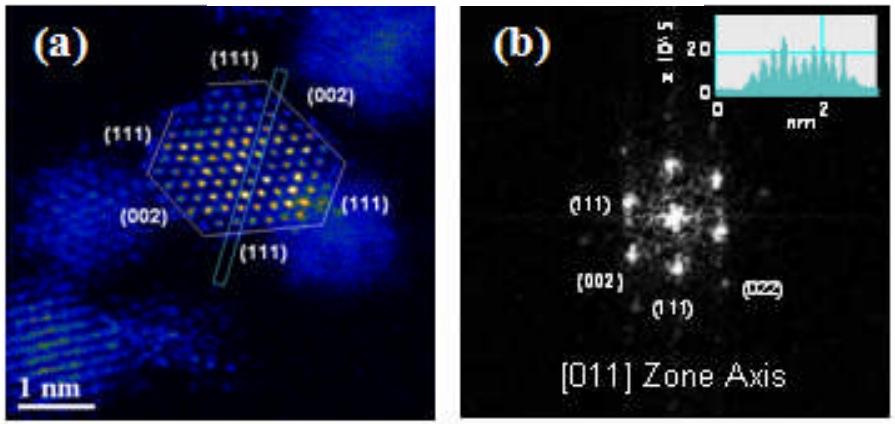

PtPd random alloy

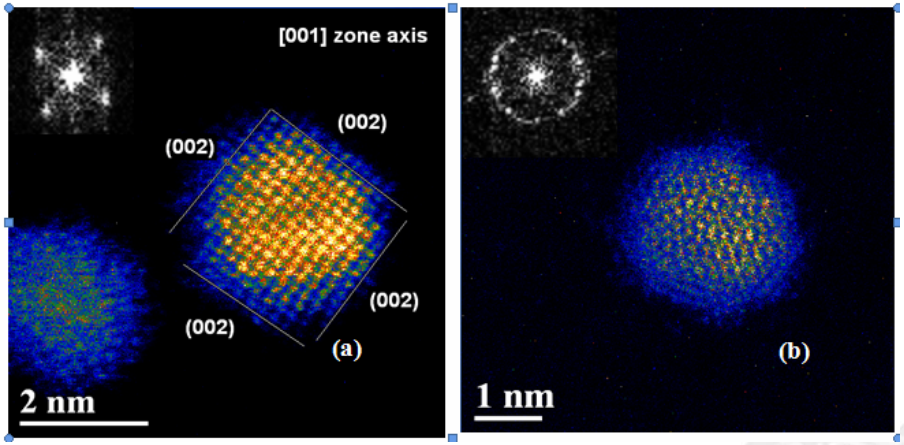

Pure Pt Pure Pd

I. Sanchez et al. *JACS* 131 (2009) 8683.

Collaboration with [illegible]

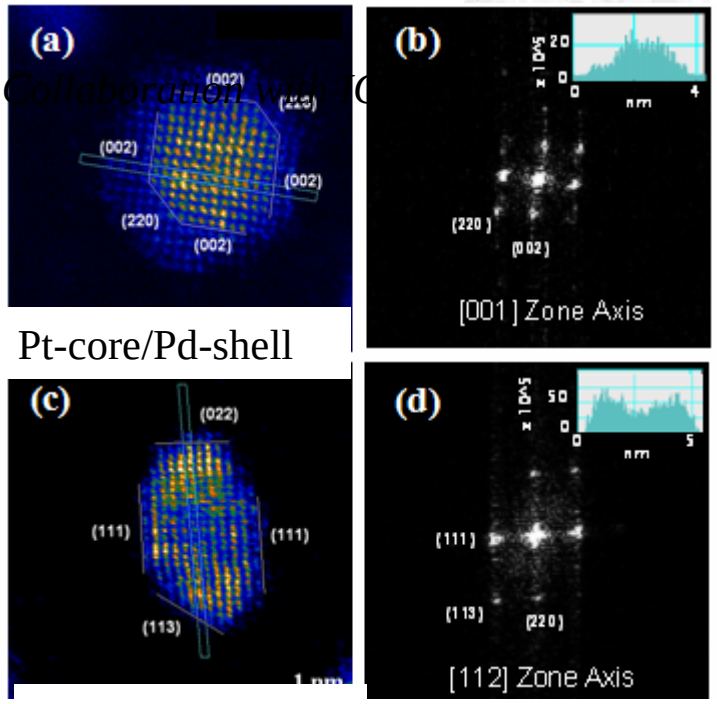

Pt-core/Pd-shell

Pd-core/Pt-shell

Cores and shells in PtPd are fcc-type but structurally incoherent !

How would this affect their properties ?

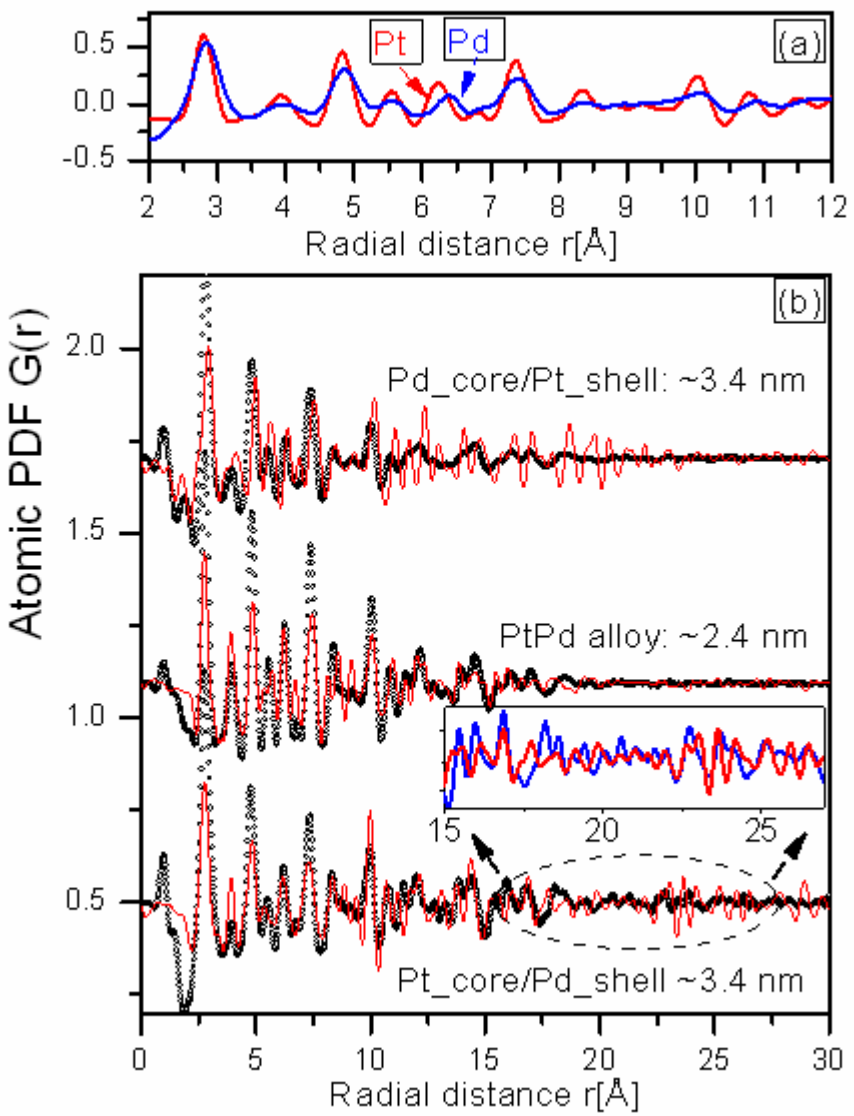

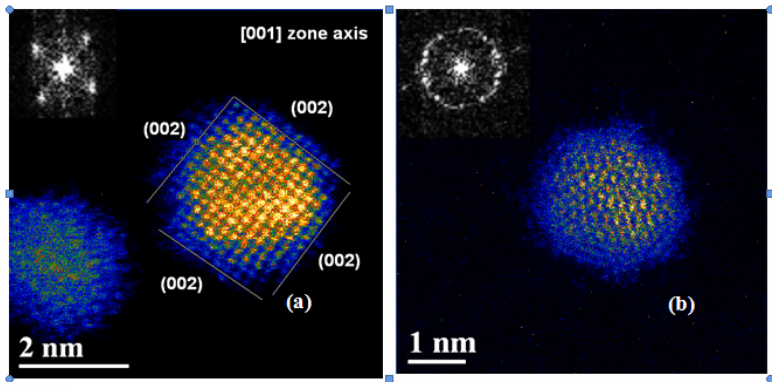

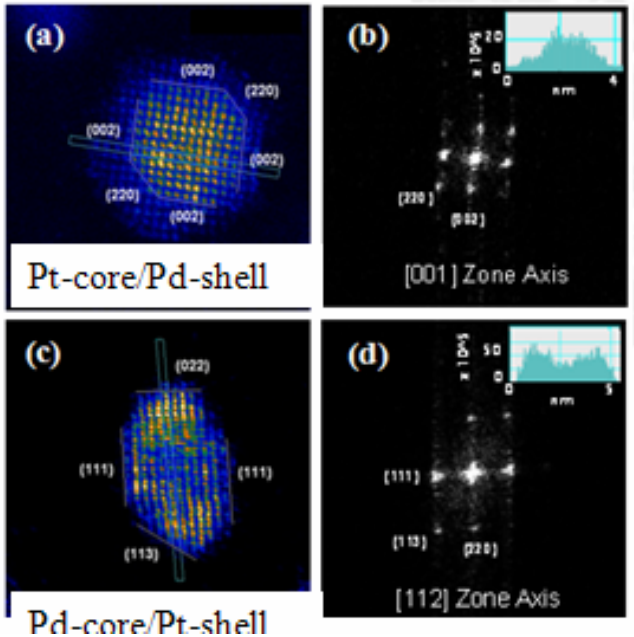

Total vs Pt differential PDFs

Resonant XRD application in pharmaceuticals:

Cisplatin

From Wikipedia, the free encyclopedia

Cisplatin, **cisplatinum**, or ***cis*-diamminedichloroplatinum(II) (CDDP)** is a platinum-based chemotherapy drug used to treat various types of cancers, including sarcomas, some carcinomas (e.g. small cell lung cancer, and ovarian cancer), lymphomas, and germ cell tumors. It was the first member of a class of anti-cancer drugs which now also includes carboplatin and oxaliplatin. These platinum complexes react *in vivo*, binding to and causing crosslinking of DNA which ultimately triggers apoptosis (programmed cell death).

Cisplatin

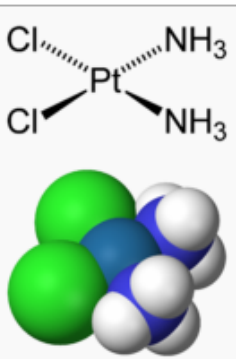

5574 *Inorg. Chem.* **1997**, *36*, 5574−5579

Structure of Amorphous Platinum Uridine Green Sulfate by AWAXS and EXAFS

Ritva Serimaa,*,† Veli Eteläniemi,† Tarja Laitalainen,‡ Arthur Bienenstock,§ Sakari Vahvaselkä,† and Timo Paakkari†

Platinum pyrimidine blues[1,2] are antitumor active, amorphous and paramagnetic products formed in reactions of cisplatin or *cis*-diaquadiammineplatinum(II) with pyrimidine bases. In several studies, e.g.,[3−7] products with varying antitumor activities, elemental compositions, and colors have been obtained. Both the detailed structures and the origin of the antitumor activity of platinum pyrimidine blues are unknown.

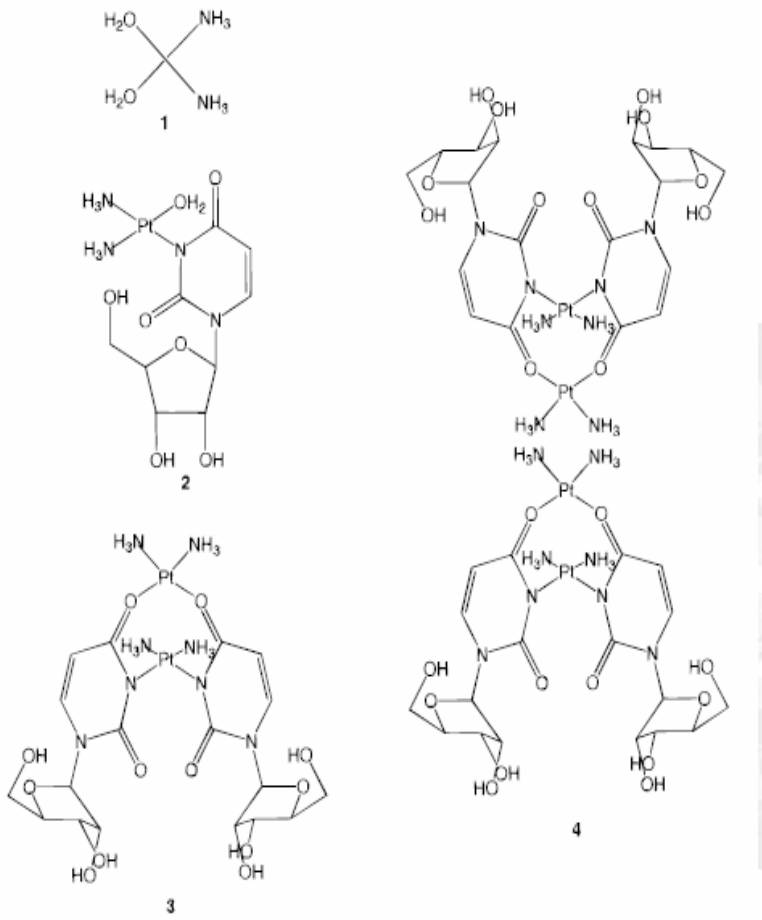

Figure 3. Assumed mononuclear (**1** and **2**), dinuclear (**3**), and tetranuclear (**4**) Pt−uridine complexes.

Traditional anti-cancer drugs……

MRI ……

Magnetic resonance imaging

From Wikipedia, the free encyclopedia
(Redirected from Magnetic Resonance Imaging)

"MRI" redirects here. For other meanings of MRI or Mri, see MRI (disambiguation).

Magnetic resonance imaging (**MRI**), or **nuclear magnetic resonance imaging** (**NMRI**), is primarily a medical imaging technique most commonly used in radiology to visualize detailed internal structure and limited function of the body. MRI provides much greater contrast between the different soft tissues of the body than computed tomography (CT) does, making it especially useful in neurological (brain), musculoskeletal, cardiovascular, and oncological (cancer) imaging. Unlike CT, it uses no ionizing radiation, but uses a powerful magnetic field to align the nuclear magnetization of (usually) hydrogen atoms in water in the body. Radio frequency (RF) fields are used to systematically alter the alignment of this magnetization, causing the hydrogen nuclei to produce a rotating magnetic field detectable by the scanner. This signal can be manipulated by additional magnetic fields to build up enough information to construct an image of the body.[1]:36

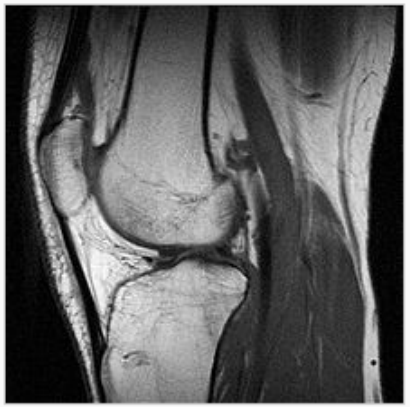

Sagittal MR image of the knee

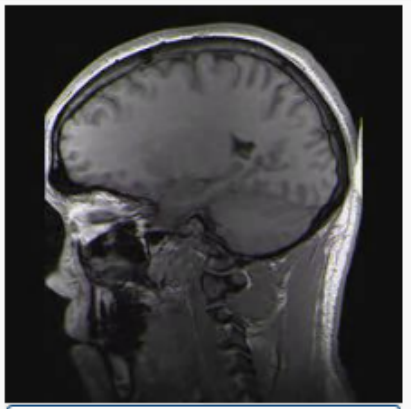

Para-sagittal MRI of the head, with aliasing artifacts (nose and forehead appear at the back of the head)

Magnetic resonance imaging is a relatively new technology. The first MR image was published in 1973[2][3] and the first cross-sectional image of a living mouse was published in January 1974.[4] The first studies performed on humans were published in 1977.[5][6] By comparison, the first human X-ray image was taken in 1895.

Magnetic resonance imaging was developed from knowledge gained in the study of nuclear magnetic resonance. In its early years the technique was referred to as nuclear magnetic resonance imaging (NMRI). However, as the word *nuclear* was associated in the public mind with ionizing radiation exposure it is generally now referred to simply as MRI. Scientists still use the term NMRI when discussing non-medical devices operating on the same principles. The term magnetic

MRI relies on contrast agents

Gadopentetic acid (in the form of **gadopentetate dimeglumine** or **Gd-DTPA**) is the first paramagnetic magnetic resonance imaging (MRI) contrast agent. First described in 1981, and introduced in 1988, it is used to assist imaging of blood vessels and of inflamed or diseased tissue where the blood vessels become 'leaky'. It is often used when viewing intracranial lesions with abnormal vascularity or abnormalities in the blood-brain barrier. It is usually injected intravenously. Gd-DTPA is a gadolinium complex of diethylenetriamine pentaacetic acid and is classed as an acyclic, ionic gadolinium contrast medium. Its paramagnetic property reduces the T1 relaxation time (and to some extent the T2 and T2* relaxation times) in NMR, which is the source of its clinical utility.

Marketed as **Magnevist** by Bayer Schering Pharma, it was the first intravenous contrast agent to become available for clinical use, and is in widespread use around the world.

Gadolinium based agents may cause a toxic reaction known as Nephrogenic Systemic Fibrosis (NSF) in patients with severe kidney problems.[1][2]

Gadopentetic acid

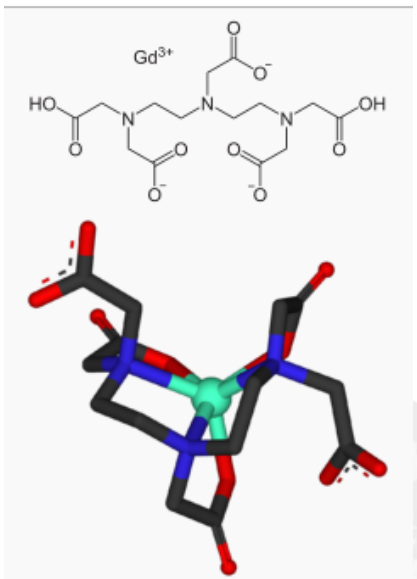

Search for better contrast agents is going on:

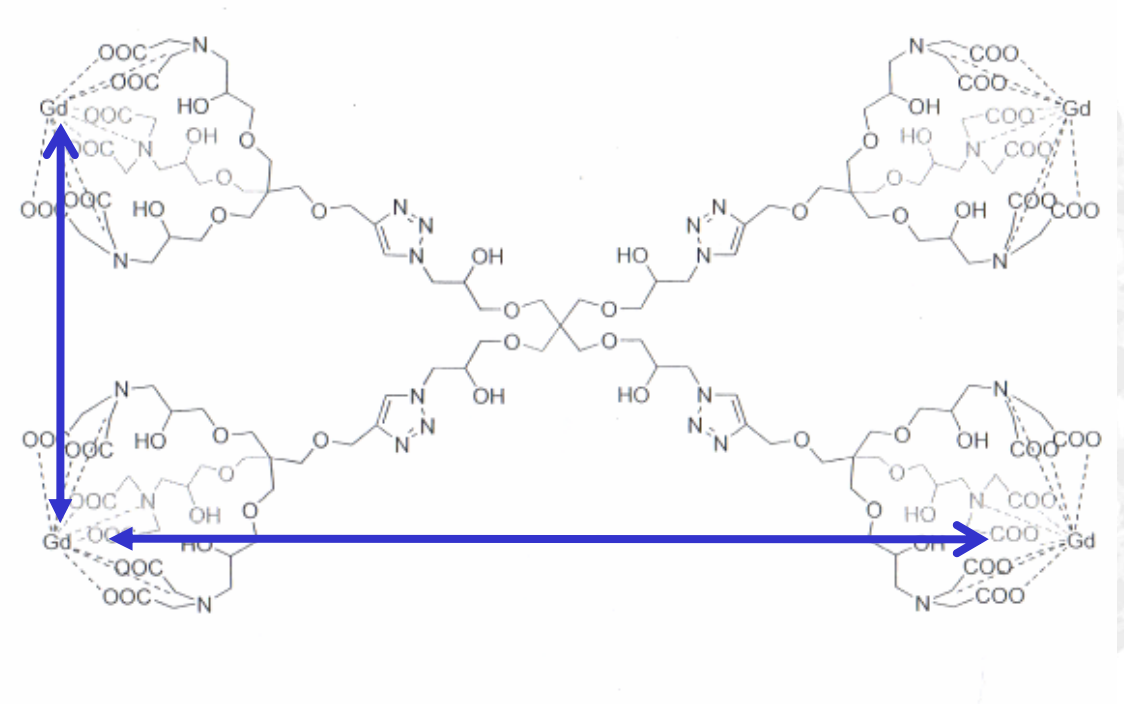

Gd-Gd pairs distribution is a critical parameter of MRI contrast agents

Gd edge resonant XRD and differential PDFs would help a lot

Collaboration with DNT

Example 6: NanoMedicine has just arrived…..

Volume 4, Issue 1, Pages 57-69 (March 2008)

previou

Fabrication of {$^{198}Au^0$} radioactive composite nanodevices and their use for nanobrachytherapy

Mohamed K. Khan, MD, PhD[a], Leah D. Minc, PhD[b], Shraddha S. Nigavekar, PhD[c], Muhammed S.T. Kariapper, PhD[a], Bindu M. Nair, PhD[a], Matthew Schipper, PhD[b], Andrew C. Cook, PhD[d], Wojciech G. Lesniak, PhD[a], Lajos P. Balogh, PhD[a]

Received 11 April 2007; accepted 26 November 2007. published online 01 February 2008.

Abstract

We describe the simple fabrication of poly({^{198}Au}) radioactive gold-dendrimer composite nanodevices in distinct sizes (diameter between 10 nm and 29 nm) for targeted radiopharmaceutical dose delivery to tumors in vivo. Irradiation of aqueous solutions of ^{197}Au containing poly(amidoamine) dendrimer tetrachloroaurate salts or {$^{197}Au^0$} gold-dendrimer nanocomposites in a nuclear reactor resulted in the formation of positively charged and soluble poly{$^{198}Au^0$} radioactive composite nanodevices (CNDs). A mouse melanoma tumor model was used to test whether the poly{$^{198}Au^0$} CNDs can deliver a therapeutic dose. A single intratumoral injection of poly{$^{198}Au^0$}$_{d=22nm}$ CNDs in phosphate-buffered saline delivering a dose of 74 μCi resulted after 8 days in a statistically significant 45% reduction in tumor volume, when compared with untreated groups and those injected with the "cold" nanodevice. No clinical toxicity was observed during the experiments. This study provides the first proof of principle that radioactive CNDs can deliver therapeutic doses to tumors.

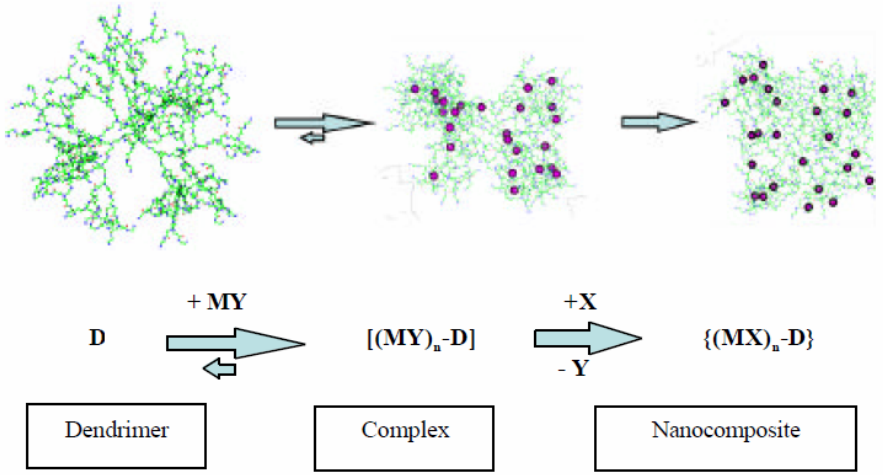

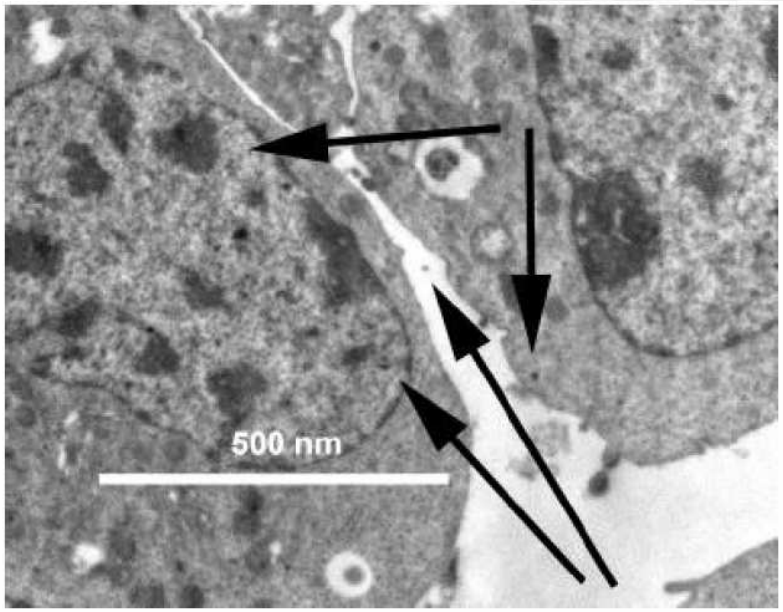

Figure 6: Electron microscope image of mouse tumor tissue 1,25 hours after {Au} injection. Unstained specimen, black dots represent gold nanocomposite clusters, dark areas within the nucleus are preferred for {Au}.

Resonant XRD can be very useful here !

Indeed atomic PDFs have proven to be very useful with nanocomposites: $(Polyaniline)_xV_2O_5nH_2O$

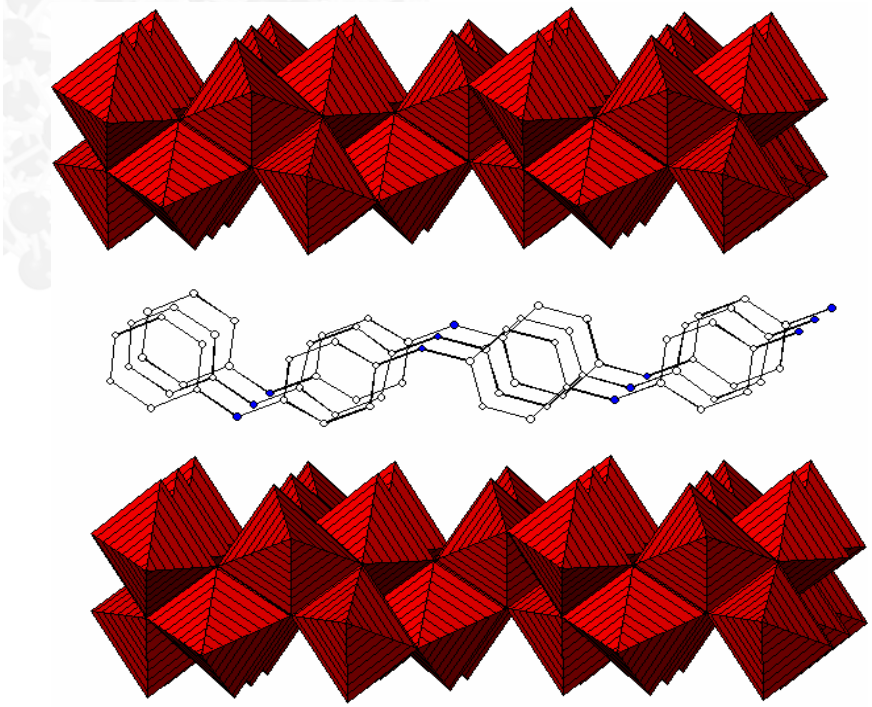

Atomic ordering in $(PANI)_xV_2O_5nH_2O$ as determined by the present PDF studies. The vanadium-oxygen octahedra (in red) are assembled in bilayers and the polyaniline chains occupy the interlayer space. The model atomic configuration is periodic and involves 476 atoms allowing theoretical studies on material's properties.

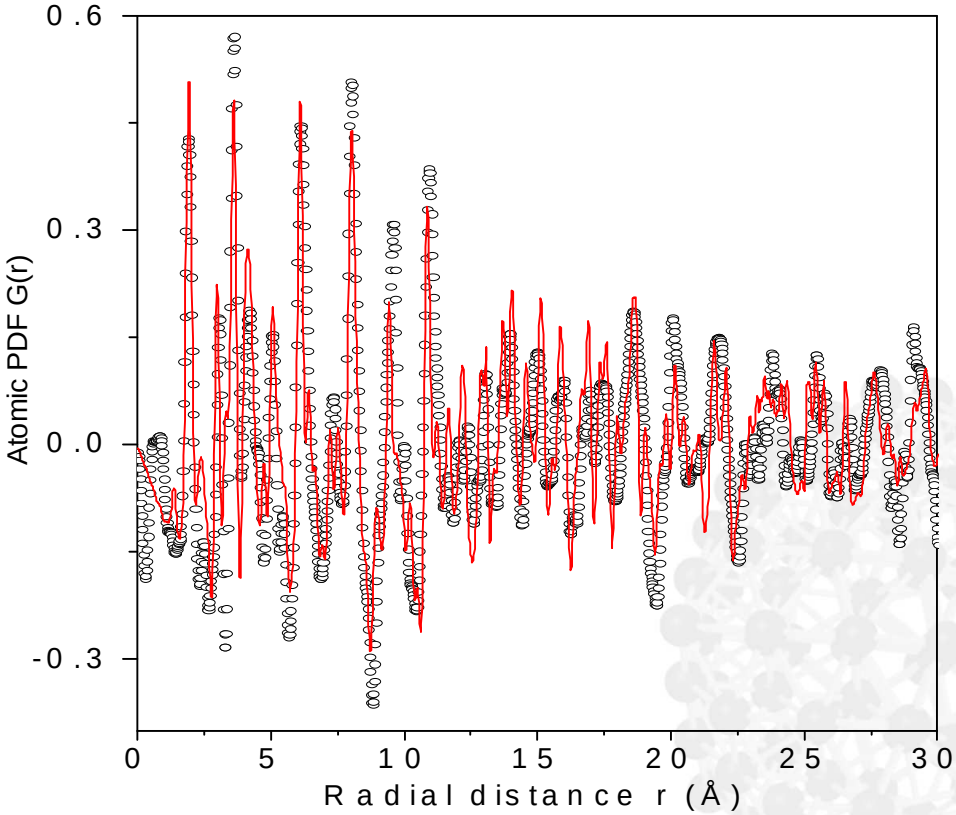

Comparison between the experimental (symbols) and model (solid line in red) PDFs for $(PANI)_xV_2O_5nH_2O$. The model PDF is calculated from the atomic configuration shown on the left.

Collaboration with M. Kanatzidis, MSU

More in Petkov et. al JACS 127 (2005) 8805.

NanoMedicine will be around for a long time…..

Porous metal–organic-framework nanoscale carriers as a potential platform for drug delivery and imaging

Patricia Horcajada[1]*, Tamim Chalati[2], Christian Serre[1], Brigitte Gillet[3], Catherine Sebrie[3], Tarek Baati[1], Jarrod F. Eubank[1], Daniela Heurtaux[1], Pascal Clayette[4], Christine Kreuz[4], Jong-San Chang[5], Young Kyu Hwang[5], Veronique Marsaud[2], Phuong-Nhi Bories[6], Luc Cynobe Sophie Gil[7], Gérard Férey[1], Patrick Couvreur[2] and Ruxandra Gref[2]*

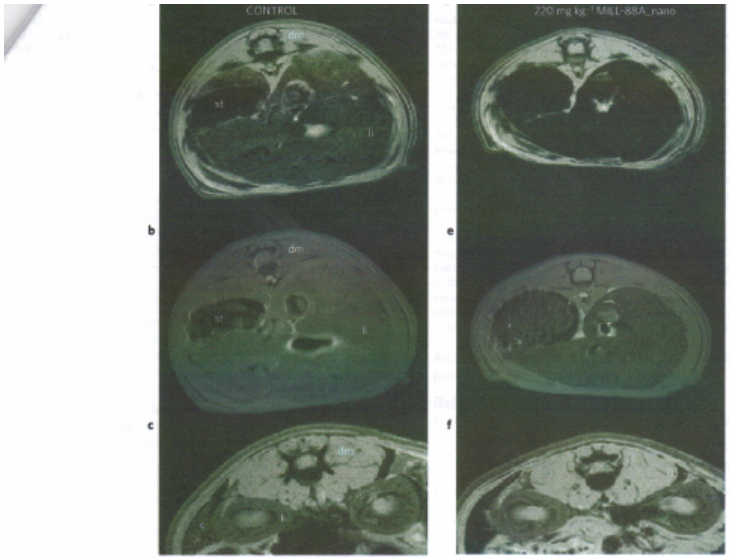

Figure 4 | Magnetic resonance images. The images were acquired with gradient echo (**a**, **c**, **d**, **f**) or spin echo (**b**, **e**) sequence of control rats (left; **a**–**c**) and rats injected with 220 mg kg^{-1} MIL-88A (right; **d**–**f**), in liver (**a**, **b**, **d**, **e**) and spleen (**c**, **f**) regions. 30 min after injection, product effect is observable on the liver and spleen. (dm, dorsal muscle; k. kidney; li, liver; s, spleen; st, stomach.)

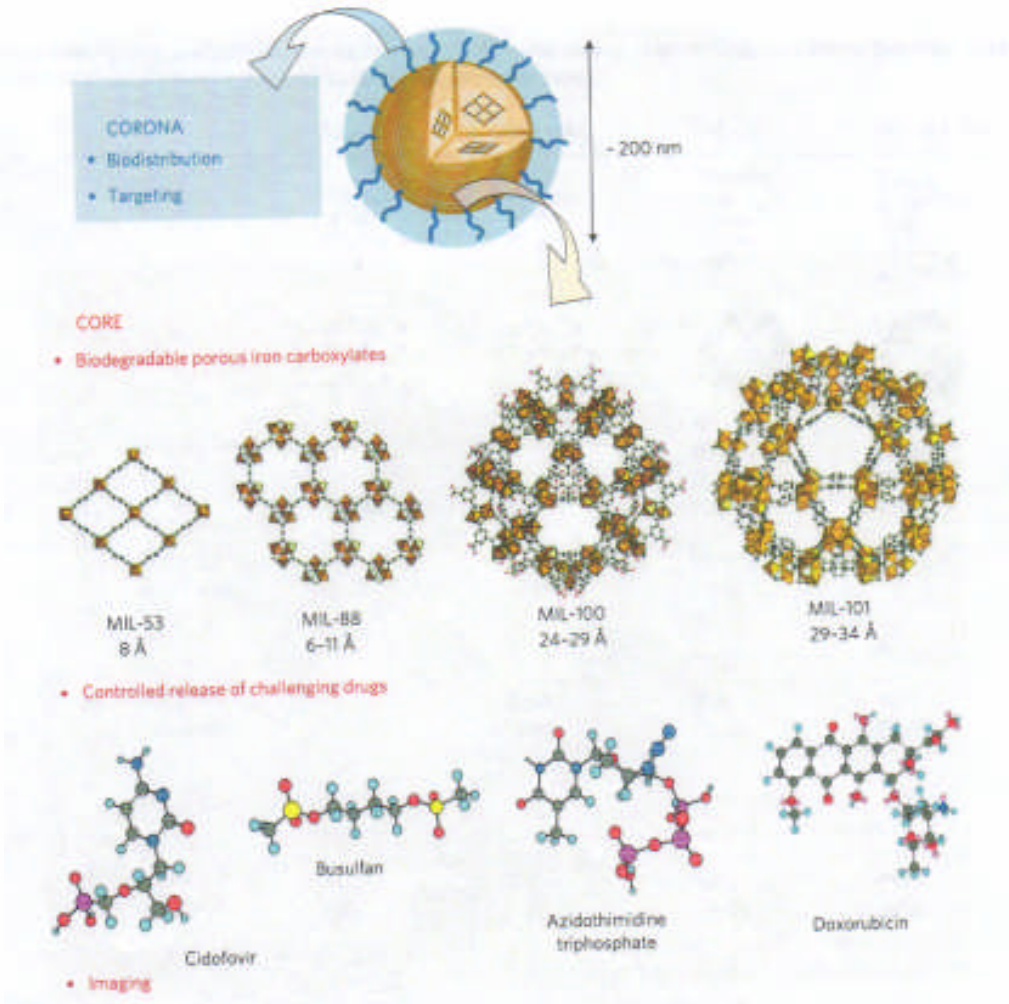

Can Atomic PDFs be used to characterize metal-organic frameworks, nanocomposites etc ?

and with metal-organic frameworks, and many more…

COMMUNICATION www.rsc.org/chemcomm | ChemComm

Direct observation of adsorbed H_2-framework interactions in the Prussian Blue analogue $Mn^{II}_3[Co^{III}(CN)_6]_2$: The relative importance of accessible coordination sites and van der Waals interactions†

Karena W. Chapman,*[a] Peter J. Chupas,*[a] Evan R. Maxey[b] and James W. Richardson[b]

Received (in Cambridge, UK) 22nd May 2006, Accepted 26th July 2006
First published as an Advance Article on the web 16th August 2006

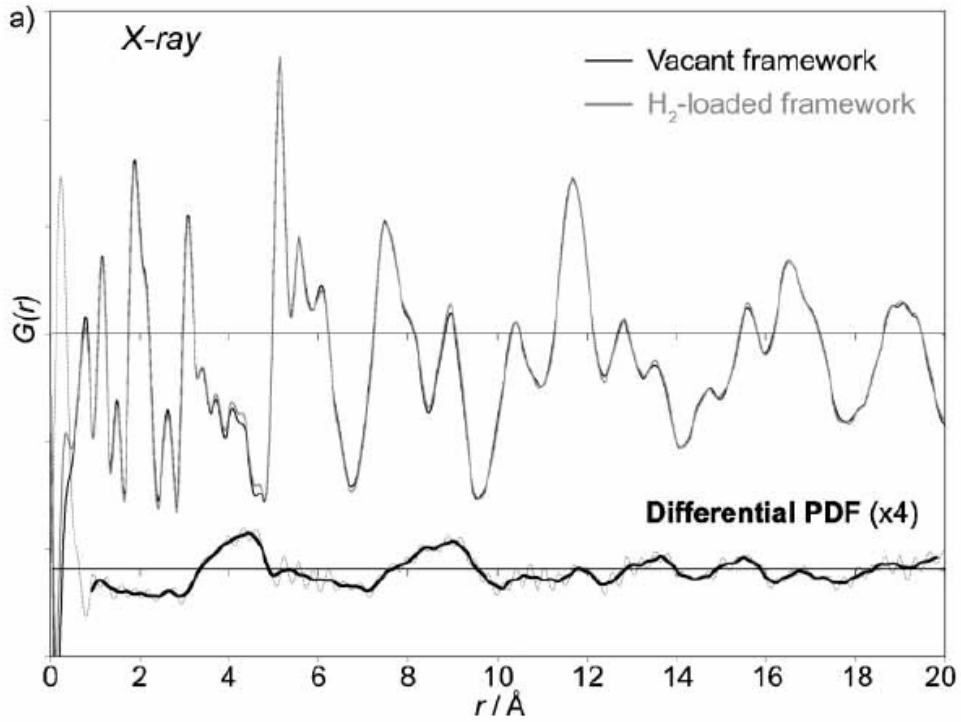

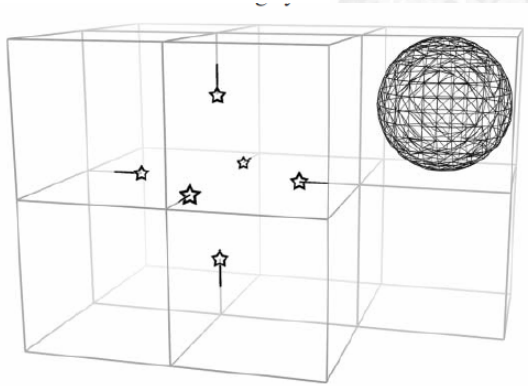

Fig. 1 Representation of the Prussian Blue network indicating the accessible Mn^{II} sites (star) surrounding a $Co(CN)_6^{3-}$ lattice vacancy. The lattice defines cavities of ~4 Å diameter connected by larger cavities associated with the aperiodic $Co(CN)_6^{3-}$ vacancies at one-third of the Co^{III} sites.

Conclusions:

Accurate structural characterization of disordered bulk and nanosized pharmaceutical materials can be done by high-energy XRD coupled to PDF (real space) data analysis. The approach succeeds because it relies on total scattering data (Bragg plus diffuse) measured over an extended range of wave vectors. It probes the material as a whole (i.e. it is not surface only sensitive/imaging like TEM) over its entire length (not only the first/second coordination sphere like EXAFS/spectroscopy) of structural coherence. It is flexible with respect to sample's state, morphology, amount, phase homogeneity and environment. Could be done using in-house or synchrotron sources of x-rays, and offer chemical specificity (resonant XRD/differential PDFs) The approach has all the potential to become a "standard structural characterization tool" in pharmaceutical research and industry.

Acknowledgements:

The work would have been impossible without the help of NSF, DoE, ARL and an army of collaborators and students ! Thank you all !

Atomic PDFs workshop coming soon:

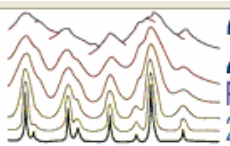

2010 Denver X-ray Conference

Plenary: The Greening of X-rays: X-rays and Renewable Energy

2-6 August 2010 - Denver Marriott Tech Center Hotel, Denver, Colorado, U.S.A.

2010 DXC Preliminary Program
Denver Marriott Tech Center Hotel, Denver, Colorado, 2 – 6 August

Plenary	Special Sessions		
	Joint XRD & XRF	**XRD**	**XRF**
The Greening of X-rays: X-rays and Renewable Energy	Cultural Heritage - Full Day New Developments in XRD & XRF Instrumentation EXAFS - NEXAFS	Stress Analysis Polymers/SAX – Full Day Micro Diffraction Rietveld Analysis Mile High Resolution XRD	Fusion and Industrial Applications of XRF Environmental and Handheld XRF Trace Analysis X-ray Imaging Quantitative Analysis

Workshops

Joint XRD & XRF	XRD	XRF
EXAFS Cultural Heritage – Full day	Trace Phase Identification using Chemical Information Texture Analysis - Full day Polymers Survey of Basic XRD Applications 2D Detectors Pair Distribution Function	Basic XRF Trace Analysis Specimen Preparation Quantitative Analysis – Full day Standards for X-ray Spectrometry